

Spatial-temporal-demand clustering for solving large-scale vehicle routing problems with time windows

Christoph Kerscher¹, Stefan Minner^{1,2}

¹Logistics and Supply Chain Management, School of Management, Technical University of Munich, Munich, Germany

²Munich Data Science Institute (MDSI), Technical University of Munich, Munich, Germany

Abstract

Several metaheuristics use decomposition and pruning strategies to solve large-scale instances of the vehicle routing problem (VRP). Those complexity reduction techniques often rely on simple, problem-specific rules. However, the growth in available data and advances in computer hardware enable data-based approaches that use machine learning (ML) to improve scalability of solution algorithms. We propose a decompose-route-improve (DRI) framework that groups customers using clustering. Its similarity metric incorporates customers' spatial, temporal, and demand data and is formulated to reflect the problem's objective function and constraints. The resulting sub-routing problems can independently be solved using any suitable algorithm. We apply pruned local search (LS) between solved subproblems to improve the overall solution. Pruning is based on customers' similarity information obtained in the decomposition phase. In a computational study, we parameterize and compare existing clustering algorithms and benchmark the DRI against the Hybrid Genetic Search (HGS) of Vidal et al. (2013). Results show that our data-based approach outperforms classic cluster-first, route-second approaches solely based on customers' spatial information. The newly introduced similarity metric forms separate sub-VRPs and improves the selection of LS moves in the improvement phase. Thus, the DRI scales existing metaheuristics to achieve high-quality solutions faster for large-scale VRPs by efficiently reducing complexity. Further, the DRI can be easily adapted to various solution methods and VRP characteristics, such as distribution of customer locations and demands, depot location, and different time window scenarios, making it a generalizable approach to solving routing problems.

Keywords clustering, spatial-temporal-demand similarity, data-based LS

1 Introduction

Given its practical relevance, numerous studies about the vehicle routing problem (VRP, Dantzig and Ramser 1959) and its variants exist (Vidal et al. 2020). Typically, rich VRPs of large-scale real-world applications are solved by heuristics. State-of-the-art metaheuristics use most of their computation time searching for local improvements in an incumbent solution by modifying customer sequences within a given tour or changing customer-vehicle assignments (Vidal et al. 2013). As the problem size increases, the number of possible local search (LS) operations grows exponentially. In response, complexity reduction techniques are applied to limit the solution space. Decomposition and aggregation methods divide the original problem into multiple smaller ones that are solved independently (Santini et al. 2023). Pruning limits the LS operators' exploration of new solutions (Arnold and Sørensen 2019). These strategies mostly follow simple rules tailored to a particular problem. In practice, however, solution algorithms must be scalable and adjustable to various problem characteristics. Thus, we propose a generalizable solution framework called decompose-route-improve (DRI) that reduces the complexity of large-scale routing problems using data-based decomposition. This approach uses unsupervised clustering to split the customers of a VRP into separate subsets. Its similarity metric combines customers' spatial, temporal, and demand features with the problem's objective function and constraints. The resulting stand-alone small-sized sub-VRPs are solved independently. The solution to the overall problem is the combination of the individual solutions of the subproblems. Finally, LS, pruned based on customers' spatial-temporal-demand similarity, resolves unfavorable routing decisions at the perimeters of the subproblems. This approach demonstrates high scalability and expeditiously achieves high-quality solutions for large-scale VRPs. Thus, our contribution to the growing research field of heuristic decomposition is twofold.

1. We formulate a novel similarity metric for unsupervised clustering to improve scalability of state-of-the-art solution methods for large-scale routing problems.
2. We tune hyperparameters of the DRI to reduce complexity based on problem attributes, i.e., size, customer characteristics, and fleet properties.

The remainder of this paper is structured as follows. Section 2 gives an overview of relevant literature. The model of the routing problem is formalized in Section 3. Section 4 presents the DRI and data-based similarity metric. Section 5 describes the computational study and numerical results, including hyperparameter setups and a benchmark against a state-of-the-art metaheuristic. Section 6 summarizes the key contributions and concludes the paper with future research directions.

2 Literature review

We present state-of-the-art solution methods and rule- and learning-based approaches to address the methods' scalability issues. At the end of this section, Table 1 classifies the reviewed methods based on the problem variant they solve, applied scalability strategies, and the solution algorithm.

2.1 State-of-the-art solution methods

In the VRP with time windows (VRPTW) (Bräysy and Gendreau 2005), delivery time windows are added to customer requests. The arrival of a vehicle at a customer is only allowed within its specified time window. Recent branch-price-and-cut algorithms can solve VRPTW instances with up to 200 customers to optimality (e.g., Costa et al. 2019, Sahin and Yaman 2022). However, several hundreds or thousands of customer requests must be fulfilled in real-world distribution scenarios. The complexity of these large-scale problems makes exact solution methods impractical. Thus, state-of-the-art solution algorithms are metaheuristics that find feasible solutions of high quality in reasonable time. Arnold et al. (2019) solve instances with up to 30,000 customers of the capacitated VRP (CVRP). The very large-scale benchmark problems are based on real-world data of Belgium's daily parcel delivery services. Once an initial solution is found using the savings heuristic by Clarke and Wright (1964) and its routes are optimized using the 2opt-heuristic by Lin and Kernighan (1973), they apply heuristic pruning exclusively based on spatial distances between customers to limit the size of the neighborhoods explored by LS. The Hybrid Genetic Search (HGS) (Vidal et al. 2012) is the most effective solver for a wide variety of small- and mid-size routing problems, including the VRPTW (Vidal et al. 2013). The HGS combines principles of genetic algorithms (GA), which create offspring solutions by crossing over its parent solutions, and inter- and intra-LS operations that try to improve the routing of that solution. Diversification and intensification of the search are achieved by an advanced population diversity management that accommodates feasible and infeasible solutions.

2.2 Scalability strategies

Santini et al. (2023) demonstrate that splitting a routing problem into a set of subproblems using unsupervised clustering and solving them recursively by the HGS improves solution quality for CVRP instances with up to 1000 customers. Their decomposition strategy is route-based following the *route-first, cluster-second (r-f, c-s)* principle and integrated repetitively, after a given number of iterations, into the HGS. Clustering is solely based on geographical distances between route centers. Bent and Van Hentenryck (2010) show that r-f, c-s decomposition based on customer information outperforms route-based separations for a large neighborhood search (LNS) heuristic. Subproblems are formed by customers within a randomly selected spatial (time) slice of the geographical plane (operational period). They report that decomposition based on customer features leads to better solutions faster. In r-f, c-s approaches, decomposition quality is limited by the incumbent route plan. This solution is found without any complexity reduction technique. Even with the implementation of decomposition techniques, LS operations consume most of the computation time (e.g., Ropke and Pisinger 2006, Vidal et al. 2013, Accorsi and Vigo 2021). Heuristic pruning improves scalability of solution algorithms that rely considerably on creating solution neighborhoods. It limits LS operators in their exploration of new solutions. The overarching goal is to find high-quality solutions faster while using less memory. Limiting the size of neighborhoods by constraining LS moves among relatively close customers is among the most widely applied pruning techniques (e.g., Helsingaun 2000, Toth and Vigo 2003, Arnold et al. 2019). However, these search limitation methodologies may exclude relevant edges, especially if routing decisions are not solely based on travel costs like in the VRPTW. Pruning that goes beyond strict rule-based restrictions is done in Beek et al. (2018) and Arnold et al. (2021). Beek et al. (2018) limit the size of their in-memory stored Static Move Descriptors (SMDs) based on their contribution to the overall objective.

Arnold et al. (2021) exploit the information of extracted routing patterns of historical solutions on LS operators for the CVRP to reduce the heuristic’s computational effort. None of the presented works combine decomposition and pruning in the solution method.

2.3 Clustering approaches

Unlike the decomposition strategies mentioned above, *cluster-first, route-second* (*c-f, r-s*) approaches decompose a routing problem into less complex subproblems before the routing step. One of the first methods following this principle is the sweep algorithm (Gillett and Miller 1974). It first assigns customers to a vehicle based on their polar angles and then does the sequencing of the individual routes. Fisher and Jaikumar (1981) heuristically solve a generalized assignment problem to assign customers to vehicles. This results in multiple traveling salesman problems (TSPs) that are solved independently. Wong and Beasley (1984) define subareas of customers to be visited based on their historical requests. Customers in the same area are served by a single vehicle. This leads to intuitive routing decisions but often to an inefficient tour plan, especially if time windows are present, as the areas are fixed once determined. Schneider et al. (2015) analyze the effect of time windows on the formation of customer districts. These territories are generated based on defined rules that take samples of the customers’ spatial and temporal information and their historical demands into account. In a second step, a tabu search (TS) heuristic solves a TSP for every customer subset. All these works have in common that the decomposition step yields stand-alone TSP problems. Thus, the clustering restricts the routing decisions as the customer allocation to a vehicle is fixed. In the clustered vehicle routing problem (CluVRP), customers are pre-assigned to clusters, and a vehicle passes to more than one cluster on its route as the sum of the customers’ demand per cluster is usually smaller than the vehicle capacity (Battarra et al. 2014). In practical applications, however, such clusters are not known in advance. Unsupervised clustering allocates customers into multiple groups based on a specified similarity metric. Jain (2010) provides a detailed summary of clustering methods most widely used, including *k*-means and its variants, hierarchical clustering algorithms like agglomerative clustering, and non-deterministic (e.g., fuzzy *c*-means) approaches that compute the degree of membership - i.e., the relative similarity - for every data object to all clusters. Yücenur and Demirel (2011) propose a genetic clustering algorithm to assign customers to depots in the multi-depot VRP (MDVRP). Ewbank et al. (2016) use a fuzzy clustering technique. The resulting TSPs are solved approximately using the nearest-neighbor (NN) and 2opt-heuristic. Qi et al. (2012) solve large-scale VRPTWs with 1000 customers using *k*-medoid clustering and the I1 heuristic by Solomon (1987). Customers are grouped into subproblems based on their pairwise spatial distance and the temporal distance between their time windows. In all these works, clustering metrics are exclusively based on the distance between customers. In contrast, our clustering metric evaluates the similarity of customers concerning the contribution to the overall problem’s objective and the consumption of the available resources when visited in sequence. Thus, our clustering is based on geographical distances between customers and their temporal and demand data.

Table 1: Overview of contributions, applied scalability strategies, and solution algorithms

	routing problem	decomposition			pruning		solution algorithm ²
		strategy	feat. ¹	subprob.	follows	feat. ¹	
Accorsi and Vigo (2021)	CVRP	-	-	-	data	s	SA+ILS
Arnold et al. (2019)	CVRP	-	-	-	rules	s	LS
Arnold et al. (2021)	CVRP	-	-	-	data	s	LS
Beek et al. (2018)	CVRP	-	-	-	data	s	LS
Bent and Van Hentenryck (2010)	VRPTW	r-f, c-s	st	VRPTW	-	-	LNS
Ewbank et al. (2016)	CVRP	c-f, r-s	s	TSP	-	-	NN+2opt
Gillett and Miller (1974)	CVRP	c-f, r-s	s	TSP	-	-	2opt
Fisher and Jaikumar (1981)	CVRP	c-f, r-s	s	TSP	-	-	B&b
Qi et al. (2012)	VRPTW	c-f, r-s	st	VRPTW	-	-	I1
Santini et al. (2023)	CVRP	r-f, c-s	s	CVRP	-	-	HGS
Schneider et al. (2015)	VRPTW	c-f, r-s	std	TSP	-	-	TS
Vidal et al. (2013)	VRPTW	r-f, c-s	s	VRPTW	rules	st	GA
Wong and Beasley (1984)	VRPTW	c-f, r-s	d	TSP	-	-	3-opt tour
Yücenur and Demirel (2011)	MDVRP	c-f	s	CVRP	-	-	-
Our approach	VRPTW	c-f, r-s	std	VRPTW	data	std	HGS-TW

¹ Features: s - spatial, t - temporal, d - demand

² Solution algorithms: B&b - branch & bound, SA+ILS - simulated annealing + iterative LS

3 Problem statement

We briefly introduce the well-known 3-index formulation of the VRPTW following Toth and Vigo (2014) to define relevant notations and equations for the description of the DRI. We consider a complete graph $G = (V, E)$. The set V includes all vertices of G . The vertices are grouped into the subset $V_c \subseteq V$, which contains n customer vertices that have to be visited, and the subset $\{w\} \subseteq V$, which consists of the depot vertex w . An edge $e_{i,j} \in E$ connects a pair of vertices $i, j \in V$ and is associated by a cost function $c_{i,j} = C(e_{i,j})$ accruing when a vehicle k directly travels from i to j . The fleet K , a set of m vehicles, is used to distribute goods stored at the depot to all customers. The capacity Q , which limits the load shipped by a vehicle k , is the same for all vehicles in K . The demand of a customer i is defined as d_i and varies over customers in V_c . The objective (1) minimizes the total travel costs. The binary decision variable $x_{i,j,k}$ indicates if vehicle k uses an edge $e_{i,j}$. Then $x_{i,j,k} = 1$, otherwise $x_{i,j,k} = 0$.

$$\min \sum_{i,j \in V} \sum_{k \in K} c_{i,j} \cdot x_{i,j,k} \quad (1)$$

The fleet size, the limited load volume of vehicles, and demand fulfillment are considered in the constraints (2) - (4). The binary decision variable $y_{i,k}$ states if a vertex i is assigned to a vehicle k . Then $y_{i,k} = 1$, otherwise $y_{i,k} = 0$.

$$\sum_{k \in K} y_{w,k} \leq m \quad (2)$$

$$\sum_{k \in K} y_{i,k} = 1 \quad \forall i \in V_c \quad (3)$$

$$\sum_{i \in V_c} d_i \cdot y_{i,k} \leq Q \quad \forall k \in K \quad (4)$$

All vehicles start and end their route at the depot (2), and every customer vertex is assigned to exactly one vehicle (3). (4) ensures that the vehicle's load does not exceed its capacity. In the VRPTW, temporal information is provided for all vertices in V . The service time s_i is needed to fulfill the order request d_i of a customer i , and the time interval $[e_i, l_i]$ restricts a customer's availability to a specific time window. Here, e_i defines the earliest possible start time of the service, and l_i is the latest allowed arrival time at a customer location. The time window of the depot $[e_w, l_w]$ defines the operational period's beginning and closing. The time variable $T_{i,k}$ defines the start of the service of k at i . Additionally, for all edges in E , the corresponding travel time $t_{i,j}$ is given.

$$e_j \leq T_{j,k} \leq l_j \quad \forall k \in K, j \in V \quad (5)$$

$$x_{i,j,k}(T_{i,k} + s_i + t_{i,j}) \leq T_{j,k} \quad \forall k \in K, i, j \in V \quad (6)$$

Delivery must start within a customer's time window $[e_j, l_j]$ (5). $T_{j,k}$ depends on the start of delivery and required service at the previous customer i plus the travel time from i to j . (6). The solution to a VRPTW instance \mathcal{J} is the set of routes $\mathfrak{R}_{\mathcal{J}} = \{R\}$. A route R is a set that represents a closed circuit that starts and ends at w and visits at least one customer vertex $i \in V_c$. Each route is assigned a single vehicle k . The set $V_R \subseteq V_c$ includes all customer vertices visited in route R . A route R is considered feasible if it does not violate (4) and (5). A vehicle may wait at a delivery point i if it arrives before the customer is available, hence $T_{i,k} < e_i$. However, the presented objective function (1) of the VRPTW only considers the direct costs of the total distance traveled based on the sum of $c_{i,j}$ of all routes of the solution $\mathfrak{R}_{\mathcal{J}}$. Let \mathfrak{P}_p be a sub-VRPTW of \mathcal{J} . Then, the overall solution is defined as the set of the individual solutions of all q subproblems, i.e. $\mathfrak{R}_{\mathcal{J}} = \{\mathfrak{R}_p\}$ where $p = 1, \dots, q$.

4 Overview of the DRI

Our approach is a three-step procedure that decomposes and solves a routing problem, and improves its solution. In the *decomposition phase*, we split \mathcal{J} based on spatial, temporal, and demand features of its vertices and edges of the underlying graph structure. An unsupervised clustering method groups the customer vertices into subsets. Each cluster represents a sub-VRPTW \mathfrak{P}_p of the same type as \mathcal{J} by adding fleet and depot data. The depot is duplicated for every \mathfrak{P}_p , and vehicles are initially allocated based on the customer demands of the clusters in relation to the overall demand. In the *routing phase*, the resulting subproblems are solved independently by a suitable method. Subsequently, in the *improvement phase*, the set of the individual route plans $\{\mathfrak{R}_1, \dots, \mathfrak{R}_q\}$ are improved using LS. Here, we focus on resolving unfavorable clustering decisions at the perimeters of the subproblems. The framework is built to solve large-scale variants of VRPTW, but its modular and generic design may enable its application to other related routing problems. The process flow of the algorithmic framework is illustrated in Figure 1.

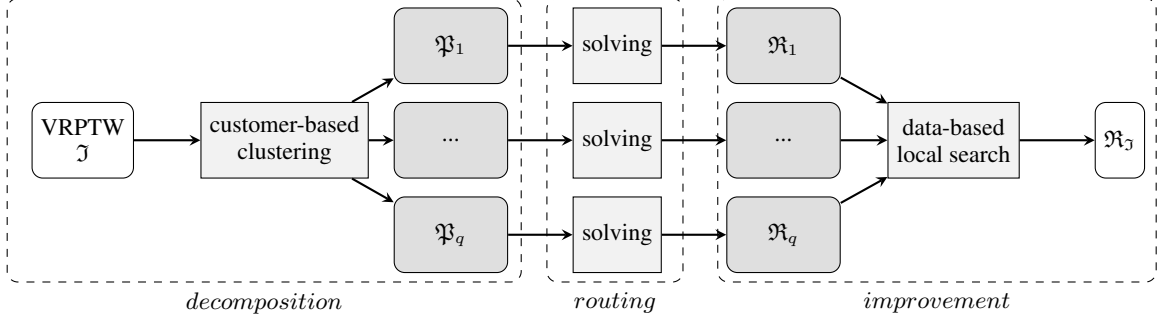


Figure 1: Overview of algorithmic framework: Decompose first, route second, improve third

4.1 Decomposition phase

The number of possible routing options increases exponentially with the number of customers involved. To achieve scalability, the DRI disregards edges that are not contributing to a good solution (i.e., are associated with high transportation costs) or can be omitted because of capacity and temporal constraints by allocating customers into separate sub-VRPTWs. In clustering, similar objects are grouped together, and dissimilar objects are allocated to different clusters. Objects are represented by features, and a clustering metric measures their similarity. In the following, we introduce these concepts in the context of the VRPTW.

4.1.1 Similarity metric:

In the DRI, the objects to be clustered are customers. A vertex $i \in V_c$ is represented by its spatial, temporal, and demand data (7).

$$\tau_i = (x_i, y_i, \theta_i, e_i, l_i, s_i, d_i) \quad (7)$$

Spatial feature data are the geographical coordinates in \mathbb{R}^2 (x_i, y_i) and the polar coordinate angle θ_i with respect to w . This allows us to include information on the relative position of customers to the depot in clustering, even when the depot is excluded from the decomposition procedure. In accordance with Gillett and Miller (1974), we calculate θ_i for every customer vertex using (8) in its range (9).

$$\theta_i = \arctan\left(\frac{y_i - y_w}{x_i - x_w}\right) \quad (8)$$

$$\theta_i = \begin{cases} (-\pi, 0) & \text{if } y_i - y_w < 0 \\ [0, \pi] & \text{if } y_i - y_w \geq 0 \end{cases} \quad (9)$$

Temporal features are $[e_i, l_i]$ and s_i . The demand feature is d_i . Clustering metrics measure similarity of objects to be clustered. In the context of routing problems, a customer pair i, j should be considered similar if $c_{i,j}$ is small and dissimilar if transportation costs are high. Let $\mathfrak{S}_{i,j}^s$ (10) be the pairwise similarity of the spatial features of customers i and j . Then, assuming that transportation costs positively correlate with the spatial distance between i and j , $F(\cdot)$ approximates the underlying cost function $C(e_{i,j})$.

$$\mathfrak{S}_{i,j}^s = F(x_i, y_i, \theta_i, x_j, y_j, \theta_j) \quad (10)$$

If temporal and demand information are present, the exclusive consideration of spatial data to measure pairwise similarity may be delusive as the constraints of a VRP drive feasibility and quality of a solution. For the VRPTW, temporal and capacity restrictions limit flexibility in routing. In particular, the likelihood of employing an edge $e_{i,j}$ in a route R is influenced by its flexibility in terms of scheduling within R . The longer period $f_{i,j}$, as defined in (11), between the closing time at j and the latest possible departure from vertex i - i.e., the sum of the opening and service time at i and travel time needed if edge $e_{i,j}$ is used - the more likely $e_{i,j}$ fits into the sequence of R . A negative value of $f_{i,j}$ indicates that $e_{i,j}$ is infeasible. It will not appear in a feasible solution as the vehicle can only serve both customers by violating one of their time windows. Figure 2 illustrates the maximum scheduling flexibility $f_{i,j}$.

$$f_{i,j} = l_j - (e_i + s_i + t_{i,j}) \quad (11)$$



Figure 2: Illustration of the maximum arrival flexibility $f_{i,j}$ in $[e_i, l_i]$

With increasing $f_{i,j}$, the possibility of waiting at a customer location before starting service increases. In (12), the minimum waiting time $h_{i,j}$ that occurs for $e_{i,j}$ is defined as the time difference between the earliest possible start date of service at j and the sum of the latest possible arrival time and the time required to fulfill service at i plus the time needed to travel from i to j . The smaller $h_{i,j}$, the less time a vehicle spends waiting at j . Figure 3 illustrates the minimum waiting time $h_{i,j}$.

$$h_{i,j} = \max\{e_j - (l_i + s_i + t_{i,j}), 0\} \quad (12)$$

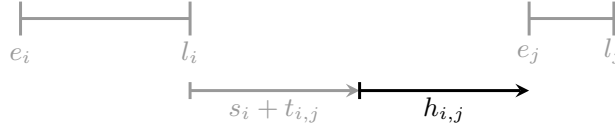


Figure 3: Minimum required waiting time $h_{i,j}$ when traveling from i to j

The decision of which customers to be routed in sequence also depends on the capacity consumption as available choices for sequencing a customer-pair into a route decrease when the loading volume utilized by its demands increases. The spatial-temporal-demand (STD) distance $\mathfrak{S}_{i,j}^{std}$ defined in (13) is the pairwise spatial distance $\mathfrak{S}_{i,j}^s$ that is proportionally penalized based on depletion of temporal and capacity resources. The lower the maximum scheduling flexibility or the higher the minimum waiting time, and the more loading capacity is utilized, the higher the penalization of the spatial distance of a customer-pair. If the relative capacity consumption of customer demands is insignificant (i.e., $\frac{d_i+d_j}{Q} \simeq 0$), both time windows $[e_i, l_i]$ and $[e_j, l_j]$ are not restrictive, and the travel time $t_{i,j}$ between the two vertices is short (i.e., $h_{i,j} = 0$ and $f_{i,j} \simeq l_w - e_w$), then $\mathfrak{S}_{i,j}^{std} \approx \mathfrak{S}_{i,j}^s \approx C(e_{i,j})$.

$$\mathfrak{S}_{i,j}^{std} = \mathfrak{S}_{i,j}^s \cdot \left(2 - \frac{f_{i,j} - h_{i,j}}{l_w - e_w} + \frac{d_i + d_j}{Q}\right) \quad (13)$$

4.1.2 Clustering algorithms:

Based on τ_i where $i \in V_c$ and $\mathfrak{S}_{i,j}^{std}$, V_c is split into q different subsets $V_c = \{V_p\}$ where $p = 1, \dots, q$. The number of clusters q is set so that the number of customers is within the range the chosen solution algorithm performs most efficiently in each subset. We define q as a hyperparameter, as no evaluation metric exists that can be used to optimize q in the context of vehicle routing. As our similarity measure is directional, i.e., $\mathfrak{S}_{i,j}^{std} \neq \mathfrak{S}_{j,i}^{std}$, but in clustering a symmetric similarity score is required, we take the minimum (14) as clustering metric. By taking the minimum, we ensure that the similarity measure always represents the arc of a pair of vertices contributing best to the underlying routing problem.

$$\overline{\mathfrak{S}}_{i,j}^{std} = \min\{\mathfrak{S}_{i,j}^{std}, \mathfrak{S}_{j,i}^{std}\} \quad (14)$$

For illustration of the DRI, we test three different clustering algorithms: partitional k -medoids and fuzzy c -medoids, and hierarchical agglomerative clustering. The well-known k -medoids clustering is used as a baseline. The fuzzy c -medoids approach is chosen, as it generates more relational data between subproblems from which the *improvement phase* can leverage. We use the medoids versions (i.e., the clusters are represented by an actual customer) as they allow for better interpretability of similarities between vertices based on $\overline{\mathfrak{S}}_{i,j}^{std}$. We implement agglomerative clustering as it mimics the NN heuristic. The algorithms and their suitability for the *decomposition phase* of the DRI are discussed in the following.

K-medoids (Park and Jun 2009) minimizes the sum of distances from the customers of each cluster to the cluster medoid m_p - i.e., the customer vertex most centrally located in the cluster.

$$\min \sum_{p=1}^q \sum_{i \in V_p} \overline{\mathfrak{S}}_{i,m_p}^{std} \quad (15)$$

Initially, q cluster medoids are defined that are most similar to all other vertices (16).

$$v_i = \sum_{j \in V_c} \frac{\overline{\mathfrak{S}}_{i,j}^{std}}{\sum_{l \in V_c} \overline{\mathfrak{S}}_{j,l}^{std}} \quad \forall i \in V_c \quad (16)$$

Subsequently, customers are assigned to clusters. A vertex i forms the cluster V_p with all vertices most similar to m_p based on $\overline{\mathfrak{S}}_{i,m_p}^{std}$. Then, the cluster medoids are updated following (17). This procedure is repeated until no medoid changes between two consecutive iterations.

$$m_p = \arg \min_{i \in V_p} \left(\sum_{j \in V_p} \overline{\mathfrak{S}}_{i,j}^{std} \right), \quad p = 1, \dots, q \quad (17)$$

The pseudocode of the k -medoids clustering is presented in Algorithm 1 in the Appendix. It is a straightforward and efficient partitional clustering approach. However, as the proposed algorithm is a local heuristic, allocating customers into subsets may vary if an alternative strategy for the initial medoids selection is chosen. We address this limitation in the *improvement phase* by refining customer allocations to routes in the overall solution.

Fuzzy c-medoids is based on fuzzy c-means of Bezdek (1981) and calculates the degree of membership μ_{i,V_p} between all a vertex-cluster combination (18).

$$\mu_{i,V_p} = \frac{1}{\sum_{g=1}^q \left(\frac{\overline{\mathfrak{S}}_{i,m_p}^{std}}{\overline{\mathfrak{S}}_{i,m_g}^{std}} \right)^{\frac{2}{\kappa-1}}} \quad (18)$$

The matrix $U = (\mu_{i,V_p})$ where $i = 1, \dots, n$ and $p = 1, \dots, q$ holds all μ_{i,V_p} . The objective in fuzzy c-medoids clustering is minimizing the variance of vertex features within clusters (19). Like in k -medoids, clusters are represented by their medoids. However, in fuzzy c-medoids, the vertices are not assigned to a specific cluster. The membership degree merely indicates a customer vertex's relative similarity to the cluster medoids. The parameter κ controls this fuzziness of clusters. For $\kappa \simeq 1$, each vertex would be assigned exactly to one cluster.

$$\min \sum_{p=1}^q \sum_{i \in V_c} \mu_{i,V_p}^{\kappa} \cdot \overline{\mathfrak{S}}_{i,m_p}^{std} \quad (19)$$

s.t.

$$\sum_{p=1}^q \mu_{i,V_p} = 1 \quad \forall i \in V_c \quad (20)$$

$$1 \leq \sum_{i=1}^n \mu_{i,V_p} \leq n - 1, \quad p = 1, \dots, q \quad (21)$$

$$\mu_{i,V_p} \in [0, 1], \quad i \in V_c, \quad p = 1, \dots, q \quad (22)$$

(20) ensures that the sum of all degrees of memberships of a vertex i is equal to 1. (21) prevents the cluster V_p from being empty or containing all vertices of V_c . The range of the degree of membership is given in (22). First, U^0 is initialized with random values. Then, each cluster's feature vector τ_p is calculated based on the weighted customer feature vectors. The q cluster medoids are selected from all customers based on the STD similarity metric to the clusters' feature vector. Subsequently, μ_{i,V_p} is updated based on $\overline{\mathfrak{S}}_{i,m_p}^{std}$. The algorithm terminates if no changes are larger than a given ϵ in U between two consecutive iterations. The pseudocode of the fuzzy c-medoids method is presented in Algorithm 2 in the Appendix. Different to k -medoids, fuzzy c-medoids performs a *soft* assignment of customers to clusters. In the *improvement phase*, this is beneficial to identify potential routing improvements faster. Since U determines the similarity of each customer to every cluster with regards to $\overline{\mathfrak{S}}_{i,m_p}^{std}$, in LS, moves can be more efficiently chosen based on the proximity data of customer vertices to other sub-routing problems. In the *routing phase*, customers must be allocated to distinct subsets to create a sub-VRPTW \mathfrak{R}_p . Therefore, we assign each vertex in V_c to cluster V_{p^*} where $p^* = \arg \max_p (\mu_{i,V_p})$ and $p = 1, \dots, q$.

Agglomerative clustering (Anderberg 1973) is a bottom-up hierarchical clustering approach. Initially, each customer $i \in V_c$ represents its own cluster V_p where $p = 1, \dots, n$, i.e., $|V_p| = 1$. Then, larger customer subsets are created by iteratively combining clusters until all vertices of V_c are allocated to q clusters. In every iteration, the cluster-pair (V_p, V_g) is merged that is most similar with regards to the STD similarity metric (23). In case of a tie, (V_p, V_g) is chosen randomly with equal probability.

$$(V_p, V_g) = \arg \min_{p,g} (\overline{\mathfrak{S}}_{V_p, V_g}^{std}), \quad p = 1, \dots, q, \quad g = 1, \dots, q, \quad p \neq g \quad (23)$$

Here, $\overline{\mathfrak{S}}_{V_p, V_g}^{std}$ depends on the linkage method that determines the customer vertices representing the clusters. In *single* linkage (24), the STD similarity of V_p and V_g equals the most similar vertex-pair $i \in V_p$ and $j \in V_g$.

$$\overline{\mathfrak{S}}_{V_p, V_g}^{std} = \min_{i \in V_p, j \in V_g} (\overline{\mathfrak{S}}_{i,j}^{std}) \quad (24)$$

Conversely, in *complete* linkage (25), $\overline{\mathfrak{S}}_{V_p, V_g}^{std}$ is equal to the similarity value of the most dissimilar vertex-pair $i \in V_p$ and $j \in V_g$ between the V_p and V_g .

$$\overline{\mathfrak{S}}_{V_p, V_g}^{std} = \max_{i \in V_p, j \in V_g} (\overline{\mathfrak{S}}_{i,j}^{std}) \quad (25)$$

In *average* linkage (26), the average of $\overline{\mathfrak{S}}_{i,j}^{std}$ between all vertex-pair combinations $i \in V_p$ and $j \in V_g$ is defined as $\overline{\mathfrak{S}}_{V_p, V_g}^{std}$.

$$\overline{\mathfrak{S}}_{V_p, V_g}^{std} = \frac{1}{|V_p| \cdot |V_g|} \sum_{i \in V_p} \sum_{j \in V_g} \overline{\mathfrak{S}}_{i,j}^{std} \quad (26)$$

The pseudocode of agglomerative clustering is presented in Algorithm 3 in the Appendix. Unlike k -medoid and fuzzy c -medoids clustering, agglomerative clustering does not depend on any initialization strategy. The formation of clusters solely depends on the chosen linkage method for the hierarchical approach. Single linkage shares similarities with the NN heuristic for routing. However, this greedy approach may unevenly allocate customers to clusters, and thus, sub-routing problems would vary significantly in size. We address this issue by adjusting the runtime limit for the different sub-VRPTWs based on the number of customers included.

4.2 Routing phase

The stand-alone routing problems \mathfrak{P}_p ($p = 1, \dots, q$) are created by duplicating the depot w for every subproblem and adding a customer subset V_p to each \mathfrak{P}_p . The total number of available vehicles m of \mathcal{J} is split across the subproblems in relation to the ratio of their demands and the total demand of the complete problem. A fleet K_p assigned to \mathfrak{P}_p is calculated using the ceiling function (27). This fleet allocation strategy is most natural, assuming K is larger than the minimum required fleet.

$$K_p = \lceil K \cdot \frac{\sum_{i \in V_p} d_i}{\sum_{i \in V_c} d_i} \rceil \quad (27)$$

In the *routing phase*, each \mathfrak{P}_p is solved separately. Ultimately, any suitable solution algorithm can be applied to generate a tour plan \mathfrak{R}_p . The overarching goal is to find near-optimal solutions with minimum required runtime. Thus, we use a state-of-the-art metaheuristics in terms of solution quality and convergence rate for small and mid-size instances of the VRPTW. Let Θ be the overall runtime limit of the DRI and ν be the time needed to create the set of subproblems $\{\mathfrak{P}_1, \dots, \mathfrak{P}_q\}$. Then, the remaining time Δ in (28) is split between the *routing* (29) and *improvement phase* (30) based on the hyperparameter α .

$$\Delta = \Theta - \nu \quad (28)$$

$$\Omega = \alpha \cdot \Delta \quad (29)$$

$$\Upsilon = (1 - \alpha) \cdot \Delta \quad (30)$$

When solved sequentially, we allocate Ω to the subproblems in relation to the ratio of their size, i.e., the number of customers in the subset p , and the size of the overall problem n using the floor function (31). Thus, the more customers in a subproblem, the more computation time is assigned in the *routing phase*.

$$\Omega_p = \lfloor \Omega \cdot \frac{V_p}{n} \rfloor \quad (31)$$

4.3 Improvement phase

In the final step of the DRI, the *improvement phase*, we apply LS to efficiently eradicate potential inefficient routes caused by the split of the customers in the *decomposition phase*.

4.3.1 Evaluating the subproblems solution quality:

We indicate whether a customer subset was solved efficiently separate from the others and which may improve when routing decisions are reconsidered by combining the route plans of the subproblems by the following measurements. Let $Z_{\mathfrak{R}_p}$ (32) be the total travel costs of route set \mathfrak{R}_p and let $\bar{Z}_{\mathfrak{R}_p}$ (33) be the average travel costs per route of \mathfrak{R}_p . Further, let u_R be the utilization of a route $R \in \mathfrak{R}_p$ (34).

$$Z_{\mathfrak{R}_p} = \sum_{R \in \mathfrak{R}_p} \sum_{e_{i,j} \in R} c_{i,j} \quad (32)$$

$$\bar{Z}_{\mathfrak{R}_p} = \frac{1}{|\mathfrak{R}_p|} Z_{\mathfrak{R}_p} \quad (33)$$

$$u_R = \frac{\sum_{i \in R} d_i}{Q} \quad (34)$$

The higher the average route costs of a solution, the more customers are involved or the longer the distances between customers. Therefore, it is less likely that the separate solution of the subproblem is efficiently contributing to the overall solution. The lower a route's utilization, the more likely it can be removed when its customers are assigned to other vehicles. Thus, LS tries to improve $R \in \mathfrak{R}_p$ with $\arg \max_p(\bar{Z}_{\mathfrak{R}_p})$ first. The routes are ordered ascendingly based on u_R . Subsequently, all routes of \mathfrak{R}_p with the next highest value of $\bar{Z}_{\mathfrak{R}_p}$ are similarly ordered. Consequently, the last route LS is applied on is $R = \arg \max_R(u_R)$ of \mathfrak{R}_p with $\arg \min_p(\bar{Z}_{\mathfrak{R}_p})$.

4.3.2 Relational data of subproblems and customers:

Assuming that the *routing phase* yields individual near-optimal solutions for all \mathfrak{P}_p , LS should focus on inter-route improvements between subproblems. Inter-route operators move a customer or a sequence of customers from one route to another, i.e., multiple routes are modified simultaneously. We prune LS moves to potentially unfavorable routing decisions between similar subproblems based on relational data obtained in the *decomposition phase*. An inter-route operation is only applied on a route pair (R, R') where $R \in \mathfrak{R}_p$ and $R' \in \mathfrak{R}_g$ and $p \neq g$. Further, \mathfrak{P}_g must lay in the vicinity Φ_p of \mathfrak{P}_p . Here, Φ_p is defined as the set of the ϕ nearest subproblems to \mathfrak{P}_p , i.e., $\Phi_p = \{\mathfrak{P}_g, g = 1, \dots, \phi\}$. The distance between two subproblems \mathfrak{P}_p and \mathfrak{P}_g is measured based on $\bar{\mathfrak{S}}_{V_p, V_g}^{std}$. On the customer level, the vicinity Φ_i is a set of the φ most similar vertices of i based on $\bar{\mathfrak{S}}_{i,j}^{std}$. If fuzzy c-medoids is used in the *decomposition phase*, LS is also educated based on the degree of membership μ_{i,V_p} where $i \in V_p, p = 1, \dots, q$. A vertex $i \in R$ is only applicable for an inter-route move if $\mu_{i,V_p} \leq \rho$ where $\rho = [0, 1]$. Consequently, moves are more focused on the borderlines of subproblems.

4.3.3 Local search:

For inter-route operations, we exemplary use *cross-over*, *relocate*, *swap*, and the *2opt*-heuristic. These operators have proven their effectiveness in previous studies (e.g., Vidal et al. 2012, Arnold et al. 2019). *Cross-over* cuts the route-pair at a certain position and swaps the tails of the routes. The *relocate* operator removes a vertex from one route and inserts it at a specific position into another. In a *swap* move, two customer vertices of different routes switch places. If an improvement is found, routes will be updated as their vertex assignment and sequencing have changed. After every successful application of an inter-route operator, an intra-route operation is applied on each updated route R^* . Intra-route operators improve a single route by modifying the sequence of the customer vertices within a route. The following intra-route operators are applicable in the DRI: *swap* and the *2opt*-heuristic. The two search strategies *first-descent* and *steepest-descent* are available for all LS operations. The first strategy accepts the first improvement of a LS operation, returns the changes in the routing, and continues with another operation until it finds no further improvement. The latter evaluates all available moves of an operation and returns the overall best before continuing with another LS operation in the next iteration. LS either stops if no further improvement can be found for all possible moves or its runtime limit Υ is reached. At the end of the *improvement phase*, all routes of the former subproblems are combined to the final tour plan of the overall problem, i.e., $\mathfrak{R}_\Upsilon = \{\mathfrak{R}_1^*, \dots, \mathfrak{R}_q^*\}$.

Figure 4 illustrates an inter-route operation for a fuzzy vertex i in R of \mathfrak{P}_4 . Its subproblem’s vicinity Φ_4 includes the sub-VRPTWs \mathfrak{P}_1 and \mathfrak{P}_2 , i.e., $\phi = 2$. Node j of route R' lays within both vicinities Φ_4 and Φ_i where $\varphi = 2$. Thus an inter-route move between $R \in \mathfrak{P}_4$ and $R' \in \mathfrak{P}_2$ is performed to evaluate the routing if a vertex j would have been assigned to \mathfrak{P}_4 rather than \mathfrak{P}_2 .

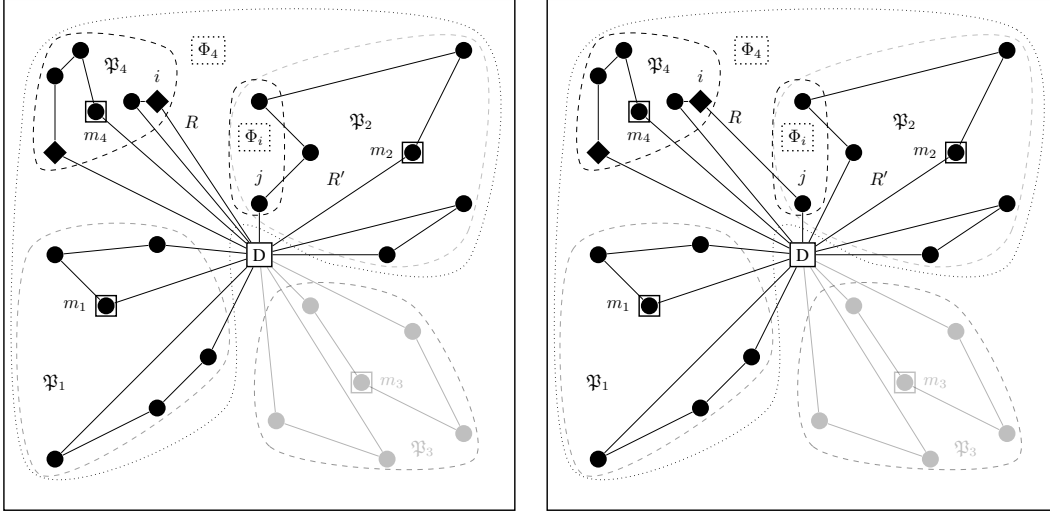


Figure 4: Illustration of a data-based inter-route move of $i \in R$ and $j \in R'$ within Φ_4 and Φ_i

5 Computational study

We perform a comprehensive numerical study to test the performance of the DRI on large-scale VRPTWs. First, we examine the impact of different problem characteristics, such as instance size, customer location distribution, and vehicle capacity, on the DRI’s hyperparameters. In the *decomposition phase*, the external parameter q is independent of the clustering approach. *Internal* parameters are κ in fuzzy c -medoids and linkage in agglomerative clustering. In the *improvement phase*, we evaluate the effect of vicinity sizes and search strategies on the efficiency of LS. Thus, we provide insights into how well the DRI can be adjusted to generate high-quality solutions for various distribution scenarios. Further, we evaluate the impact of customer features on the solution and how the *decomposition* and *improvement phase* leverage from this data. In particular, we compare the introduced similarity metric $\mathfrak{S}_{i,j}^{std}$ against a baseline clustering metric and measure the effect of data-based LS against rule-based approaches. Additionally, we investigate the influence of budgeting the computation time between the *routing* and *improvement phase*. Finally, we benchmark our results against the HGS-TW implementation by Kool et al. (2022) (<https://pyvrp.org/>).

5.1 Dataset and test environment

We use the 180 large-scale VRPTW instances with 600 – 1000 customers of Gehring and Homberger (1999). The instances are distinguished concerning spatial distribution of customers in clustered (C), random (R), and random-clustered instances (RC). Further, C1, R1, and RC1 instances have a short operational period (i.e., a smaller time difference between the closing and opening time of the depot) and tight capacity restrictions for the vehicles. In contrast, C2, R2, and RC2 instances are characterized by a high vehicle capacity and an extended operational period. Thus, more customers are visited within a route, and the routes are long. The time-window scenarios range from very restrictive time windows for all customers to 75% customer time windows with almost no limiting effect. All experiments are run on a single thread of an Intel(R) Xeon(R) Platinum 8160 CPU 2.1 GHz processor with 2.8GB of RAM running Ubuntu 20.04 LTS. The DRI framework is implemented in Python 3.9 and calls the HGS-TW implemented in C++ and LS operations implemented in Julia 1.8.2.

5.2 Hyperparameters - decomposition phase

For the autonomous analyses of the *decomposition phase*’s hyperparameters, we terminate the DRI after the *routing phase*. The subproblems are solved using the HGS-TW. Its termination criterion is set to 5,000 successive iterations performed without improvement to achieve sufficient convergence of the algorithm.

5.2.1 External parameters:

The number of subproblems q the VRPTW is split into directly impacts routing flexibility. Most *cluster-first, route-second* approaches create subproblems that are served by a single vehicle. Thus, q is determined based on the minimum required fleet size to serve all customers, i.e., fleet-based. The solver-based approach sets q such that the number of customers in the subproblems can be solved efficiently, i.e., close to optimality in reasonable time, by the chosen solution algorithm. Previous studies show that the HGS-TW performs best on problems with less than 500 customers. Figure 5 shows that the solver-based approach leads, on average, to lower costs for all instance types. The fleet-based approach fails to identify good subproblems when customers are randomly located. If customers are located in clusters, and routes are short, i.e., C1 instances, more subproblems lead only to slightly worse solutions.

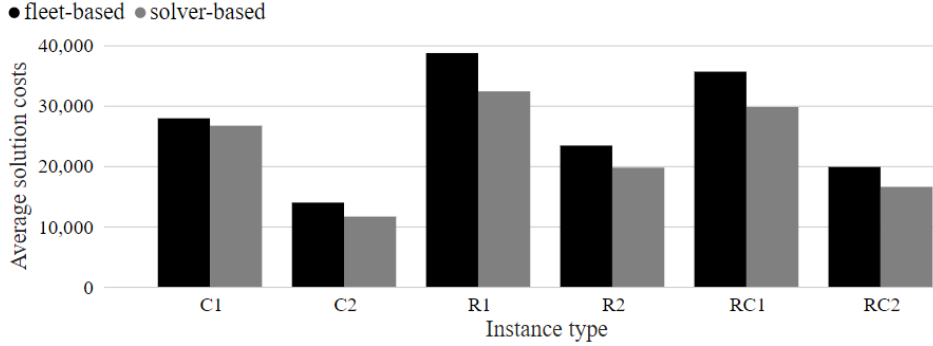


Figure 5: Impact of the strategy to determine q on the routing costs

The pair-wise spatial similarity $\mathfrak{S}_{i,j}^s$ estimates the travel cost function $C(e_{i,j})$ based on the customers' spatial features. In the Gehring and Homberger (1999) benchmark instances, $C(e_{i,j})$ is equal to the Euclidean distance between a vertex pair, and $c_{i,j} = t_{i,j}$. Accordingly, we specify $\mathfrak{S}_{i,j}^s$ as follows.

$$\mathfrak{S}_{i,j}^s = \sqrt{(x_j - x_i)^2 + (y_j - y_i)^2 + \lambda \cdot (\theta_j - \theta_i)^2} \quad (35)$$

The parameter λ controls the weight of the relative position of a customer to the depot when determining spatial similarity of customers. For $\lambda = 0$, $\mathfrak{S}_{i,j}^s = C(e_{i,j})$. If $\lambda = 1$, the difference between the coordinates and the difference in the customer-depot angle are equally weighted. Accordingly, if $\lambda = 2$, the difference in customers' polar angles to the depot is given twice the importance compared to the distance between their coordinates. Figure 6 shows that adding relative depot information, on average, improves the cluster creation concerning routing costs, even when spatial similarity could exactly represent travel costs. The rationale behind this is that when including the customer-depot angle, the form of the clusters is wedge-shaped, which follows the natural shape of cost-minimal routes. The relatively small improvement can be ascribed to the characteristic of the Gehring and Homberger (1999) instances that the depot is always located in the customers' geographical center. When the depot is decentral, θ_i is of higher importance.

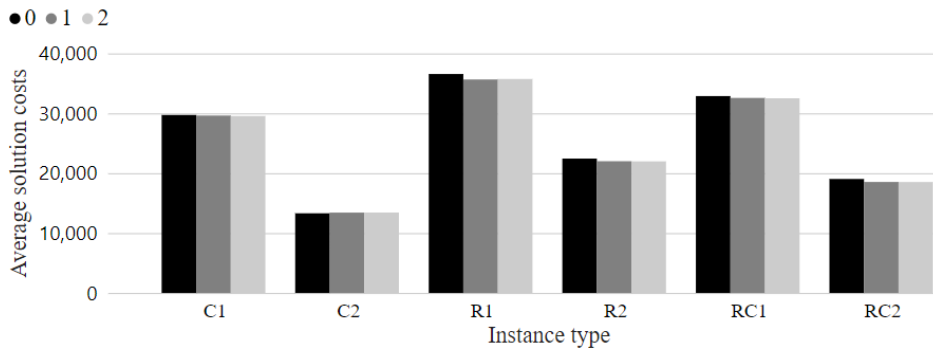


Figure 6: Impact of the vertex depot angle weighting factor $\lambda = \{0, 1, 2\}$ on the routing costs

5.2.2 Internal parameters:

We first analyze approach-specific parameters before we compare the clustering algorithms introduced in 4.1.2. In fuzzy clustering, κ , the parameter that controls the fuzziness of the clusters, is usually set to 2 (Bezdek 1981). The higher κ , the more fuzzy the clusters are. Figure 7 shows that the solution costs of the *decomposition* and *routing phase* are not very sensitive to different values for κ for different customer, vehicle capacity, or time window characteristics. That is a consequence of the design of the DRL, where we assign each customer to a single subproblem. In fuzzy c-medoids, a customer is assigned to that cluster where its degree of membership value is maximum. In agglomerative clustering,

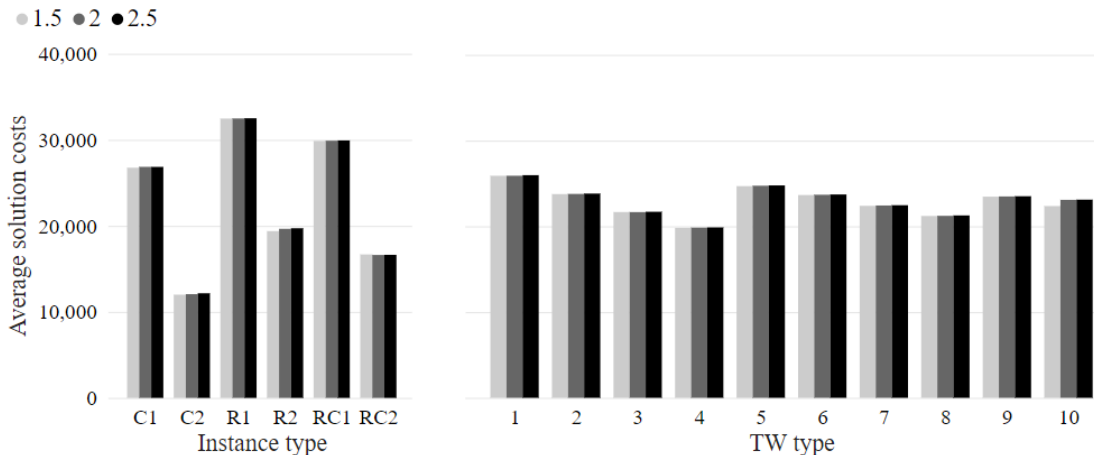


Figure 7: Impact of $\kappa = \{1.5, 2, 2.5\}$ in fuzzy c-medoids on the routing costs

the formation of the clusters depends on the linkage method. In Section 4.1.2, we presented *single*, *complete*, and *average* linkage. Figure 8 shows that *single* linkage only works well for C instances where customers are in dense areas sparsely distributed around the depot. Thus, combining customers following the principle of the NN heuristic leads to high-quality sub-VRPTWs. That is also true when the time windows are tight, i.e., TW type 1. This time window scenario makes the routes short and compact, as most routing options over a longer distance are infeasible. For all other instance and TW types, *average* and *complete* linkage result in lower solution costs. The poor performance of the *single* linkage is interesting, as it also fails to efficiently reduce the size of the edge set E (i.e., distance matrix) as shown in Figure 9. The complexity reduction is calculated as the sum of the subproblems' edge sets size $|E_p|$ relative to the size of the edge set of the original problem E , i.e., $|E|^{-1} \cdot \sum_{p=1}^q |E_p|$. Theoretically, a less reduced distance matrix leads to more routing options and better route plans (when runtime is not a limiting factor). The more clusters are created, the higher the possible reduction of the edge set size. However, *single* linkage tends to form one large subproblem of almost the same size as the original problem, while other subproblems only consist of a few customers. That is because of its greedy strategy that combines clusters solely based on the most similar customer pair, leading to an unfavorable structure of the subproblems. The linkage methods *complete* and *average* form evenly sized subproblems and thus achieve similar reduction scores. Thus, we disregard *single* linkage in the following analyses.

5.2.3 Impact of similarity metric in the decomposition phase:

Figure 10 compares the results when decomposing the original instance based on $\mathfrak{S}_{i,j}^{std}$ using the complete feature vector τ_i against the baseline metric $C(e_{i,j})$. This baseline is highly competitive, as, by definition, travel costs are the primary driver of solution quality. Our results show that the STD metric is, on average, superior for all problem characteristics. Thus, it is beneficial to use spatial information in combination with temporal and demand data to measure customer similarity and effectively group customers into separate subsets in the *decomposition phase*. Table 2 lists the solution of the best run of each clustering method and q for instances that include 1000 customers. We only report routing costs for time window scenarios 1, 10, 4, and 6 to improve readability. Bold values represent the best solution per row. For C instances, agglomerative clustering constantly yields the best solution, regardless of whether the routes are short (C1) or long (C2) or different time window scenarios are active. For C1 instances, solution costs increase slightly with increasing q . Thus, agglomerative clustering can efficiently separate C1 instances into multiple subproblems. Therefore, these instances show high scalability potential as their relatively short routes do not spread over the complete spatial plane.

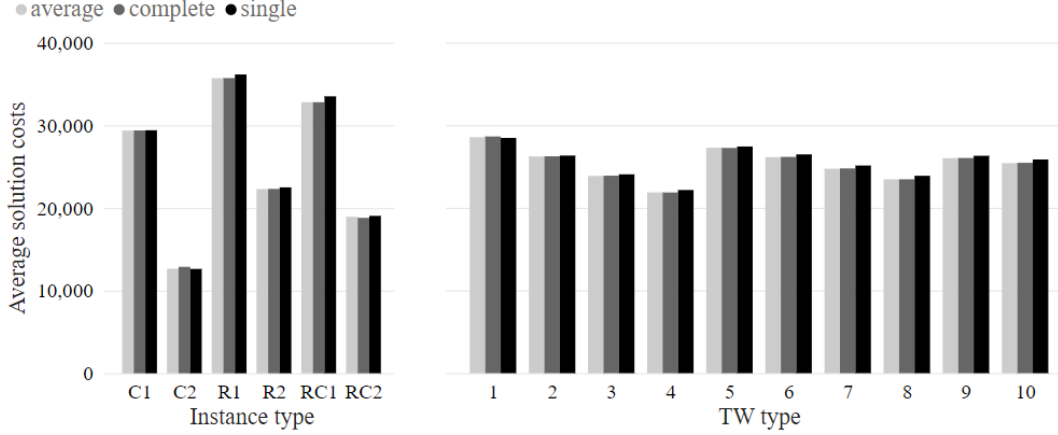


Figure 8: Impact of linkage methods in agglomerative clustering on the routing costs

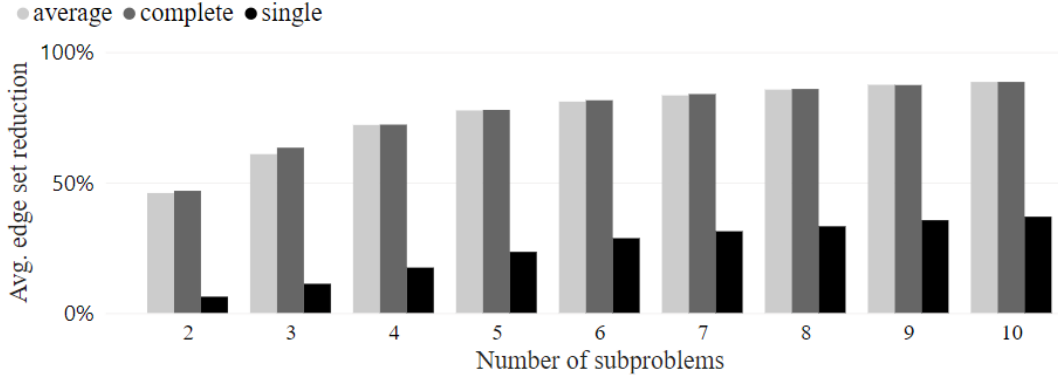


Figure 9: Impact of linkage methods in agglomerative clustering on the reduction of the edge set

Thus, additional splits do not worsen the final solution quality even when the size of E is reduced by up to 80%, i.e., $q = 6$. For C2 instances, transportation costs slightly increase with the number of clusters. That is mainly because longer routes make it difficult to efficiently separate many subproblems. For R2 instances, k-medoids constantly achieves the best results as the size of the clusters is well-balanced. For R1 and RC1 instances, agglomerative clustering and k-medoids achieve similar results. Similar to C1 instances, more clusters can be created without downgrading the solution significantly. Among the three clustering algorithms, fuzzy c-medoids only finds the overall best solution once (instance RC2_10_6). Hence, deterministic clustering is superior in the context of decomposing routing problems. This result is not surprising as we have to allocate each customer to a single subproblem. The fuzzy information is particularly relevant for LS operations in the *improvement phase*.

5.3 Hyperparameters - improvement phase

The impact of the *improvement phase* depends on the clusters created by the *decomposition phase* and their solutions found by the *routing phase*. The fewer subproblems and the more runtime allocated to them, the better their solutions, making it harder to find improvements when combining the separate route plans. However, for an autonomous evaluation of the impact of hyperparameters in the *improvement phase*, the solutions of the subproblems yielded by the *routing phase* should include unfavorable routing decisions for the overall solution. This is achieved by splitting instances into many subproblems and setting short runtimes for solving. Thus, we consider instances with 1000 customers, set $q = 10$ in the *decomposition phase*, and $\Omega = 60$ seconds in the *routing phase*. This computation time is shared between the subproblems proportionally to their size, i.e., a cluster p with 100 customers must be solved in $\Omega_p = 6$ seconds, and the stopping criterion Ω_g for a cluster g with, e.g., 120, is 7 seconds.

Table 2: Solution costs of agglomerative clustering (ac), fuzzy c-medoids (fcm), and k-medoids (k-m) for different number of subproblems q

q	2			3			4			5			6		
	ac	fcm	k-m	ac	fcm	k-m	ac	fcm	k-m	ac	fcm	k-m	ac	fcm	k-m
C1_10_1	42,479	42,876	42,783	42,479	43,270	42,479	42,479	42,550	42,481	42,482	43,236	42,499	42,487	43,351	42,753
C1_10_10	40,200	40,621	40,438	40,210	40,873	40,365	40,174	40,711	40,369	40,115	41,044	40,494	40,087	41,080	40,222
C1_10_4	39,695	39,969	39,798	39,658	39,990	39,692	39,646	40,079	39,750	39,642	40,278	39,940	39,734	40,397	39,912
C1_10_6	42,471	42,768	42,471	42,471	43,541	42,471	42,471	43,565	42,491	42,474	44,510	42,472	42,479	44,809	43,282
C2_10_1	16,879	17,603	17,277	16,950	18,429	17,629	16,973	18,875	17,703	16,973	18,338	18,104	17,034	18,193	18,542
C2_10_10	15,813	16,120	15,962	15,892	16,872	15,938	15,947	16,811	16,114	15,963	17,088	16,490	16,104	16,764	16,753
C2_10_4	15,589	15,774	15,690	15,672	16,407	15,704	15,702	16,283	15,623	15,724	16,742	15,978	15,846	16,195	16,430
C2_10_6	16,362	16,816	16,531	16,434	17,560	16,826	16,459	17,869	17,281	16,476	17,851	17,067	16,583	17,382	17,423
R1_10_1	54,462	54,427	54,570	54,216	54,506	54,495	54,207	54,536	54,220	54,350	54,811	54,736	54,879	55,713	55,242
R1_10_10	48,450	48,337	48,427	48,514	48,368	48,403	48,512	48,405	48,215	48,814	48,343	48,221	48,934	49,398	48,450
R1_10_4	43,137	43,158	43,049	43,050	43,111	43,142	42,989	43,170	43,009	43,056	43,179	43,224	43,157	43,707	43,217
R1_10_6	48,121	48,251	48,027	48,005	48,292	47,845	47,924	48,056	47,877	48,100	48,146	47,931	48,226	48,788	47,909
R2_10_1	37,827	37,638	37,449	38,117	37,901	37,630	38,374	39,887	37,792	39,166	39,775	38,259	39,661	40,494	38,604
R2_10_10	31,049	30,774	30,769	31,231	30,881	30,940	31,395	32,582	30,943	32,166	32,571	31,590	32,583	32,732	33,004
R2_10_4	18,603	18,461	18,245	18,634	18,330	18,359	18,756	19,629	18,319	19,153	19,459	18,663	19,572	19,894	18,858
R2_10_6	30,321	30,166	29,818	30,401	30,124	30,014	30,597	31,873	29,970	31,395	31,679	30,303	31,845	32,451	30,701
RC1_10_1	46,597	46,669	46,629	46,581	46,839	46,690	46,571	46,620	46,585	46,729	46,654	46,733	46,740	47,073	47,004
RC1_10_10	44,105	44,438	44,078	44,129	44,512	44,259	44,257	44,274	44,246	44,249	44,632	44,311	44,316	44,972	44,422
RC1_10_4	41,920	42,018	41,866	41,786	42,076	41,960	41,852	42,124	42,042	41,873	42,188	42,178	41,815	42,679	42,138
RC1_10_6	45,596	46,028	45,689	45,657	46,076	45,673	45,801	45,863	45,698	45,782	46,247	45,690	45,858	46,573	45,951
RC2_10_1	28,527	28,725	28,747	29,038	29,734	28,635	29,369	29,616	29,000	29,648	30,576	29,194	30,081	30,970	29,558
RC2_10_10	22,306	22,307	22,248	22,619	23,285	22,421	22,765	23,057	22,855	22,930	23,729	23,147	23,255	24,227	24,092
RC2_10_4	15,985	16,008	16,014	16,259	16,876	16,164	16,538	16,630	16,361	16,655	17,327	16,537	16,839	17,725	16,960
RC2_10_6	26,397	26,372	26,387	26,794	27,504	26,420	26,982	27,273	26,608	27,160	28,107	26,896	27,521	28,493	27,094

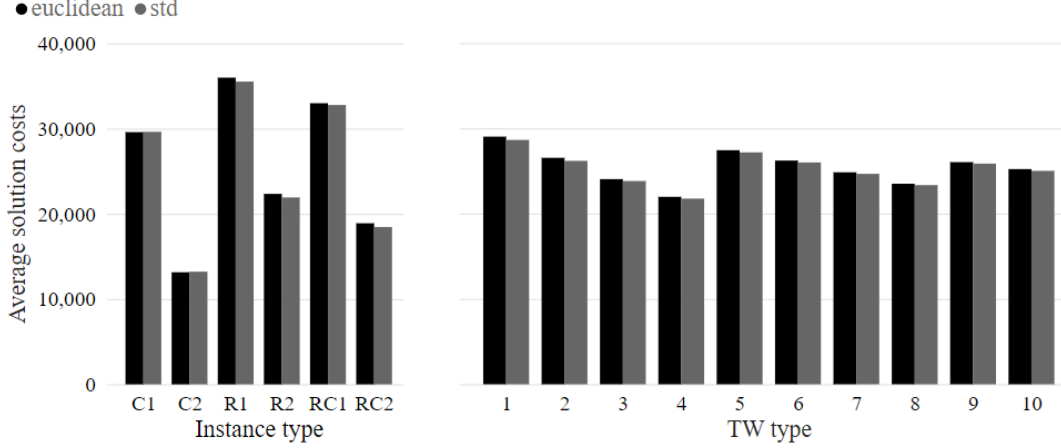


Figure 10: Impact of the similarity metric ($\mathfrak{S}_{i,j}^{std}$) on the routing costs in comparison to the baseline ($C(e_{i,j})$)

5.3.1 Internal parameters:

We calculate the relative difference of the error gap $\xi_{\mathfrak{R}_T}$ ($\xi_{\mathfrak{R}_T}^l$) before (after) the *improvement phase* in (36). The *error gap* (37) is defined as the relative difference between the total cost of the solution generated $Z_{\mathfrak{R}_T}$ and the total costs of the best known solution (BKS) $Z_{\mathfrak{R}_T^*}$. BKS solutions of all benchmark instances are obtained from the CVRPLIB website at <http://vrp.atd-lab.inf.puc-rio.br/index.php/en/> (Accessed on October 1st, 2023).

$$\tilde{\xi} = \frac{\xi_{\mathfrak{R}_T}^l - \xi_{\mathfrak{R}_T}}{\xi_{\mathfrak{R}_T}} \quad (36)$$

$$\xi_{\mathfrak{R}_T} = \frac{Z_{\mathfrak{R}_T} - Z_{\mathfrak{R}_T^*}}{Z_{\mathfrak{R}_T^*}} \quad (37)$$

The effectiveness (i.e., achieved improvement of the overall solution \mathfrak{R}_T , and the runtime until a local optimum is reached) is mainly driven by the pruning factors ϕ , i.e., the number of route-pairs available for LS, and φ , i.e., the number of vertices available for a specific LS move. The parameter ϕ defines the number of subproblems in Φ_p . Thus, ϕ limits the number of route-pairs considered in LS. Figure 11 and Figure 12 report the impact of $\phi = \{1, 3, 5, 7, 9\}$ on the LS efficiency. For $\phi = 9$, no route-pairs are excluded as $q = 10$. With increasing ϕ , the overall solution is improving on average. This effect reaches a plateau for $\phi = 5$. Also, the runtime increases as LS moves are applied on more route-pairs but without leading to noteworthy further improvements.

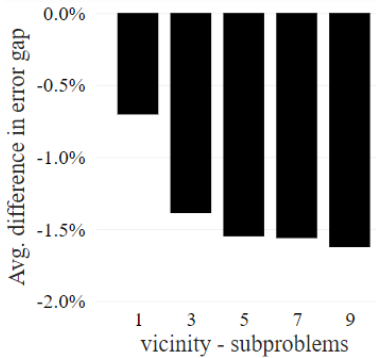


Figure 11: Impact of Φ on error gap

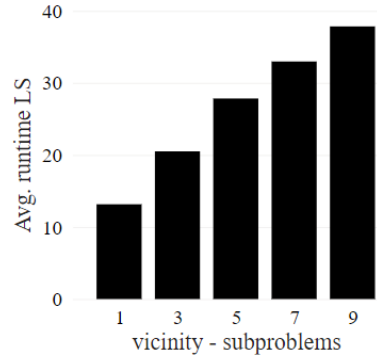


Figure 12: Impact of Φ on LS runtime

The parameter φ sets the size of the vicinity Φ_i on the vertex level. Thus, it limits the number of moves possible in a LS operation. Figure 13 reports the average $\tilde{\xi}$ and Figure 14 shows the average runtime of the *improvement phase* for $\varphi = \{5, 10, 30, 1000\}$. If $\varphi = 1000$, no pruning is active. When the goal solely is to compensate for potentially inefficient routing decisions along the perimeters of the subproblems fast, on average, it is sufficient to limit LS moves to the 10 most similar vertices. For smaller φ , a local optimum is reached faster.

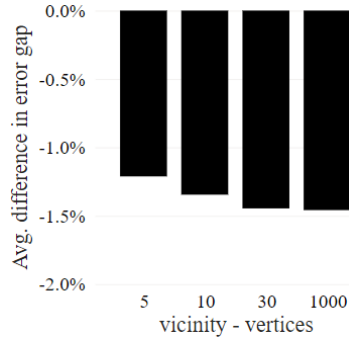


Figure 13: Impact of φ on error gap

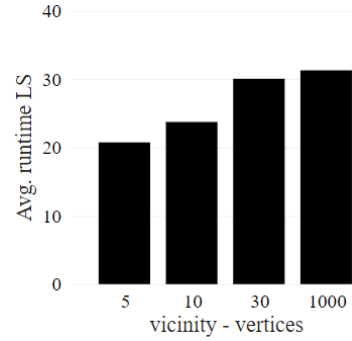


Figure 14: Impact of φ on LS runtime

Table 3 lists the average reduction in error gap and average computation time for the two LS strategies *first-descent* and *steepest-descent* for different customer location distributions. *Steepest-descent* is superior in improving a solution, particularly when customers are randomly located, i.e., R and RC. Thus, evaluating all available moves of a LS operator reduces the risk of getting stuck in a local optimum too early. The more moves are executed, the longer LS runs. However, on average, computation time of the *steepest-descent* increases not proportionally with average solution improvement.

Table 3: Impact of search strategy on LS efficiency

customer location distribution	first-descent		steepest-descent	
	Avg. $\tilde{\xi}$	Avg. Υ	Avg. $\tilde{\xi}$	Avg. Υ
C	-0.74%	38.54	-0.86%	36.76
R	-0.31%	41.56	-1.14%	67.08
RC	-1.51%	69.95	-2.73%	78.28

5.3.2 Impact of data-based approach in improvement phase:

Our data-based approach aims to guide LS in the *improvement phase*. To achieve efficient pruning, it is essential to carefully select the vertices of Φ_i . Typically, one would select the most promising vertices to the solution, i.e., based on $C(e_{i,j})$. However, Figure 15 and Figure 16 show that using the STD distance that includes the penalization based on feasibility improves the efficiency of LS in comparison to the Euclidean distance between the customer coordinates. When fuzzy c-medoids is used in the *decomposition phase*, we receive additional information about customers' degree of membership to subproblems. Fuzzy vertices are located along the boundaries of neighboring clusters. A customer i is labeled fuzzy when $\arg \max_{V_p} (\mu_{i,V_p}) < \rho$. For $\rho < 1$, LS moves are pruned exclusively to such fuzzy customers.

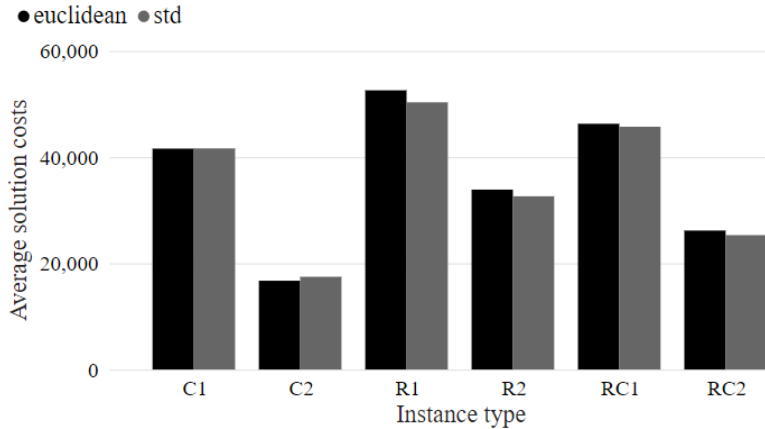


Figure 15: Impact of the of the similarity metric $\mathfrak{S}_{i,j}^{std}$ on the LS efficiency - routing costs

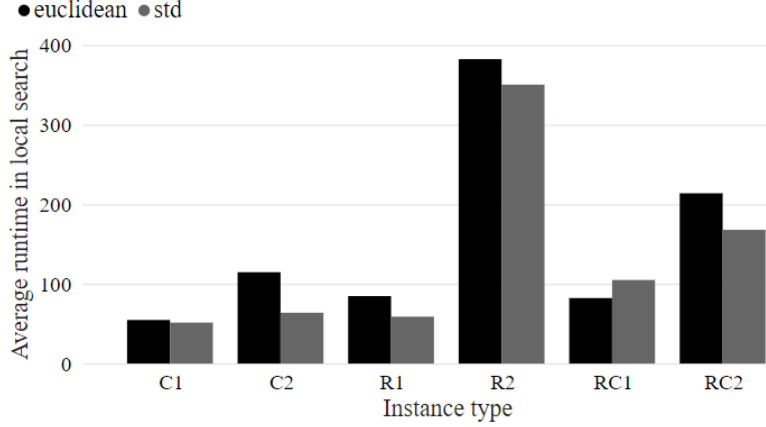


Figure 16: Impact of the of the similarity metric $\mathfrak{S}_{i,j}^{std}$ on the LS efficiency - runtime

Figure 17 shows improvements even when the threshold is strict, i.e., $\rho \leq 0.5$. The more customers are marked fuzzy, i.e., the larger ρ , the more LS operations are executed and the better the final solution. However, Figure 18 shows that the runtime grows exponentially with increasing ρ , indicating that most modifications appear near neighboring subproblems' perimeters. Thus, data-based LS that leverages information obtained from the *decomposition phase* is particularly beneficial when the available computation time for the *improvement phase* is short.

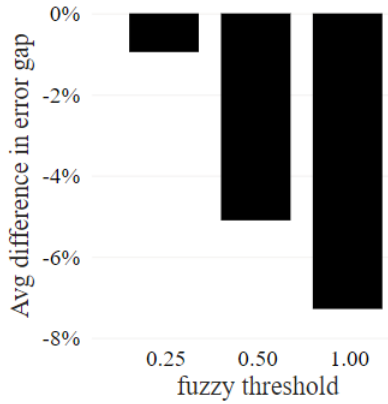


Figure 17: Impact of ρ on error gap improvement

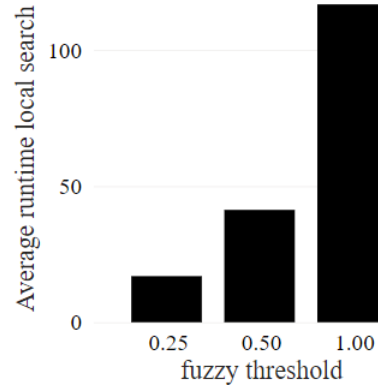


Figure 18: Impact of ρ on LS runtime

5.3.3 Runtime budgeting in DRI:

As introduced in Section 4.2, the computation time must be allocated between the three phases of the DRI, i.e., *decomposition*, *routing*, and *improvement*. Even for large instances with 1000 customers, the clustering barely consumes any runtime, i.e., $\nu \leq 0.5$ seconds. Thus, we focus on the runtime split $\alpha = \{0.75, 0.8, 0.9\}$ of the available time between the *routing* (α) and *improvement phase* ($1 - \alpha$). LS aims to revise the solution found in the previous steps. Thus, we allocate most computation time to the *routing phase*. The hyperparameters are set based on the analyses presented in the previous sections and are listed in Table 4. Two total runtime limits are applied: $\Delta = \{30, 300\}$. Figure 19 shows that the shorter the total runtime and the fewer clusters are created, the more runtime should be allocated to the *routing phase*. Here, spending more time to solve the subproblems allows us to find better solutions than running an exhaustive LS between the subproblems. With increasing runtime and more subproblems created, reserving more time for the *improvement phase* is beneficial. Then, the subproblems are likely to be solved close to optimality, and more improvements can be found in the regions where the customers have been split.

Table 4: DRI hyperparameter setup for computational time budgeting analysis

hyperparameter	values
number of clusters θ_i	{2, 5, 10} 1
clustering method	k-medoids, agglomerative clustering
similarity metric	$\mathfrak{S}_{i,j}^{std}$
ϕ	5
φ	10
search strategy	<i>steepest-descent</i>

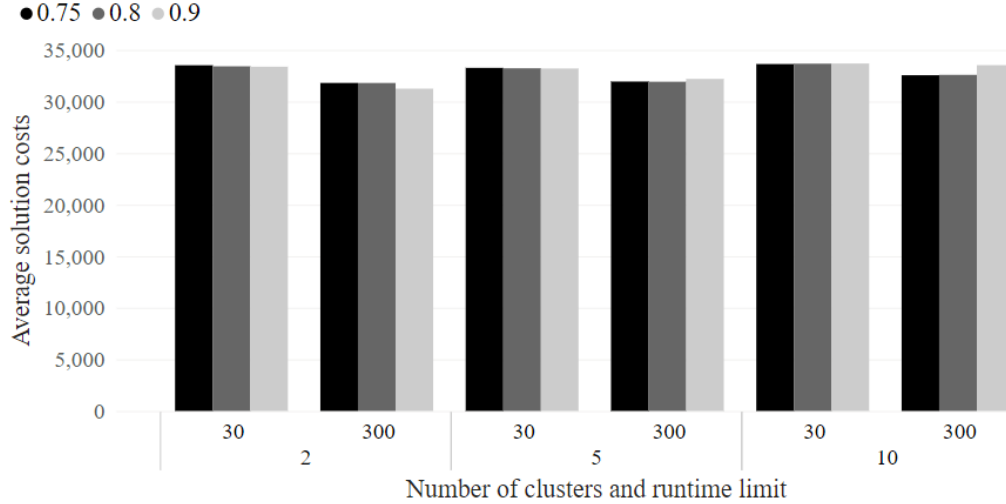


Figure 19: Impact of the runtime allocation α on the routing costs

5.3.4 Comparison against state-of-the-art solver:

We compare the DRI framework with the standard HGS-TW implementation (<https://pyvrp.org/>) to evaluate its potential to increase scalability of state-of-the-art solution methods. Therefore, we compare the quality of the solution of the two algorithms after specific runtimes. Here, the focus lies on short computation times, as our goal is to develop a solution that finds solutions of high-quality fast. Thus, we set $\Theta = \{15, 30, 45, 60, 75, 90, 120, 300\}$. Table 5 lists the average of the best solutions found for different instance sizes per instance and time window type. The bold values highlight the best solution per runtime limit and instance. Tables 6, 7, and 8 in the Appendix list the best solutions found for the instances with 600, 800, 1000 customers respectively. On average, the DRI outperforms the HGS-TW for most instances for $\Theta \leq 60$. When routes are short (C1, R1, RC1), splitting instances into multiple smaller subproblems, routing them separately, and applying data-based LS outperforms the standard HGS-TW over all tested runtimes. Table 6 shows that for C instances with 600 customers, the HGS-TW converges within 60 seconds. Thus, decomposition does not improve scalability for this instance type for medium-sized problems. However, the DRI finds better solutions for the R and RC instances for short runtimes, i.e., $\Theta = \{15, 30\}$. With increasing problem sizes (Tables 8 and 7), the DRI reveals its strength in scaling state-of-the-art solution algorithms.

6 Conclusion

We developed the DRI to efficiently solve large routing problems. It combines data-based decomposition and pruning strategies with state-of-the-art routing methods. The computational study demonstrates that our proposed similarity metric, which includes customers' spatial, temporal, and demand information and reflects the problem's objective function and constraints, outperforms classic clustering metrics solely based on customer locations. Pruning is more efficient when the STD metric limits LS moves compared to a metric based only on travel costs. Our approach effectively addresses scalability issues of common heuristics.

Table 5: Comparison of solution quality between DRI and HGS-TW for different runtimes

J-type	TW	Θ	15		30		45		60		75		90		120		300	
			DRI	HGS	DRI	HGS	DRI	HGS	DRI	HGS	DRI	HGS	DRI	HGS	DRI	HGS	DRI	HGS
C1	1	1	27,428	27,253	27,428	27,253	27,428	27,253	27,428	27,253	27,428	27,253	27,428	27,253	27,428	27,253	27,428	27,253
C1	10	10	26,733	27,251	26,478	26,846	26,446	26,648	26,390	26,648	26,363	26,545	26,371	26,504	26,289	26,437	26,139	26,281
C1	4	4	26,373	27,123	26,205	26,650	26,191	26,519	26,124	26,400	26,043	26,337	26,026	26,326	25,971	26,313	25,824	25,927
C1	6	6	27,351	27,250	27,351	27,241	27,351	27,240	27,351	27,240	27,351	27,240	27,351	27,240	27,351	27,240	27,351	27,240
C2	1	1	12,722	13,053	12,577	12,282	12,575	12,256	12,575	12,105	12,575	12,105	12,575	12,105	12,575	12,105	12,575	12,105
C2	10	10	12,090	13,112	11,692	12,150	11,647	11,708	11,550	11,602	11,431	11,557	11,402	11,546	11,347	11,514	11,324	
C2	4	4	11,882	12,416	11,392	11,869	11,367	11,577	11,330	11,460	11,256	11,301	11,205	11,262	11,105	11,220	11,056	
C2	6	6	12,519	13,048	12,102	11,943	12,080	11,804	12,062	11,747	12,045	11,740	12,050	11,733	12,041	11,723	12,038	11,718
R1	1	1	39,371	117,926	38,645	117,441	38,410	117,165	38,326	117,078	38,252	38,552	38,133	38,342	38,069	38,115	37,781	37,759
R1	10	10	33,756	33,907	33,452	33,746	33,399	33,521	33,239	33,350	33,077	33,208	33,006	33,128	32,852	33,036	32,559	32,757
R1	4	4	30,074	30,462	29,920	30,109	29,871	29,962	29,791	29,905	29,757	29,833	29,676	29,782	29,496	29,672	29,135	29,262
R1	6	6	33,810	34,073	33,616	33,823	33,474	33,676	33,345	33,561	33,327	33,494	33,239	33,385	33,105	33,204	32,696	32,878
R2	1	1	27,363	28,376	26,811	27,216	26,598	26,716	26,544	26,544	26,512	26,462	26,318	26,356	26,284	26,285	26,064	25,881
R2	10	10	22,382	22,578	21,746	21,878	21,679	21,677	21,505	21,552	21,393	21,429	21,328	21,342	21,291	21,223	21,128	20,883
R2	4	4	13,973	14,284	13,716	13,978	13,673	13,784	13,608	13,675	13,479	13,640	13,465	13,585	13,381	13,497	13,289	13,248
R2	6	6	22,051	22,446	21,515	21,913	21,392	21,658	21,280	21,465	21,176	21,329	21,150	21,208	21,017	21,109	20,801	20,846
RC1	1	1	32,525	32,862	32,232	32,593	32,077	32,373	31,957	32,272	31,942	32,094	31,846	32,050	31,807	31,890	31,531	31,610
RC1	10	10	30,498	30,852	30,231	30,498	30,114	30,341	30,052	30,246	30,012	30,177	29,920	30,115	29,801	29,952	29,560	29,660
RC1	4	4	28,782	28,982	28,529	28,820	28,504	28,697	28,447	28,617	28,380	28,535	28,349	28,499	28,197	28,397	28,034	28,098
RC1	6	6	31,799	32,058	31,423	31,645	31,382	31,497	31,237	31,370	31,145	31,229	31,052	31,220	30,969	31,123	30,684	30,819
RC2	1	1	21,217	22,686	20,642	21,401	20,527	20,900	20,409	20,700	20,364	20,512	20,326	20,335	20,301	20,150	20,178	19,918
RC2	10	10	16,311	16,540	15,810	15,986	15,760	15,727	15,731	15,651	15,619	15,532	15,586	15,494	15,514	15,425	15,382	15,223
RC2	4	4	12,119	12,490	11,831	12,207	11,746	11,899	11,715	11,781	11,668	11,711	11,638	11,659	11,605	11,560	11,491	11,376
RC2	6	6	19,501	20,363	18,803	19,529	18,661	19,019	18,612	18,730	18,527	18,575	18,486	18,505	18,404	18,335	18,308	18,110

In the DRI, the more customers served, the more subproblems are formed, and the computation effort is shifted towards the *improvement phase*. The edge set is most reducible, i.e., the DRI forms more subproblems, when customers are located closely together in sparsely distributed areas and routes are short. Fewer subproblems are required if the customers' distribution pattern is random and routes are long. Thus, if a feasible, high-quality solution needs to be generated fast for large-scale routing problems, the DRI outperforms current state-of-the-art solution algorithms. In the current setup, the LS only accepts strict improvements. Thus, it is not possible to escape local optima. Metaheuristics, i.e., simulated annealing or TS, can be used for complete improvement. As our goal is to focus on explicit route improvements, we refrain from implementing more complex search strategies in the improvement phase. The cost function is solely calculated by the Euclidean distance between two vertices in the benchmark datasets. Investigating how the DRI performs on more complex cost functions that (i) consider the total driving time of the vehicles, i.e., also includes the waiting and service time at a customer location, and (ii) retrieves real-world travel data for a more sophisticated cost evaluation could yield valuable insights. Further, we plan to extend the DRI to other problem attributes, e.g., a heterogeneous fleet, multiple depots, and pickup and delivery requests.

Acknowledgement

The authors thank Anne Kibler, Roger Kowalewski, Marilena Leichter, and Heiner Zille from SAP SE for their helpful insights during the project. Moreover, the authors would like to thank Elif Erden and Jan Eichhorn for their help in coding the LS library. The research of Christoph Kerscher and Stefan Minner has been supported by SAP SE.

Appendix

Algorithm 1 k -medoids

- 1: Initialization: Select q customer vertices following (16) as initial medoids.
 - 2: **repeat**
 - 3: Assign each vertex i to the closest cluster V_{p^*} , where $p^* = \arg \min_p (\overline{\mathfrak{S}}_{i,m_p}^{std})$.
 - 4: Set customer i that is most similar to all customers of that cluster as new medoid following (17).
 - 5: **until** $\{m_p, p = 1, \dots, q\}_t = \{m_p, p = 1, \dots, q\}_{t+1}$
 - 6: **return** set of customer clusters $\{V_p\}$, $p = 1, \dots, q$
-

Algorithm 2 fuzzy c -medoids

- 1: Initialization: U^0
 - 2: **while** $U^r - U^{r-1} < \epsilon$ **do** ▷ Convergence of the degrees of membership
 - 3: $\tau_p = \sum_{i=1}^n \mu_{i,V_p} \cdot \tau_i$, $p = 1, \dots, q$
 - 4: $m_p = \arg \min_{i \in V_c} (\overline{\mathfrak{S}}_{i,p}^{std})$, $p = 1, \dots, q$
 - 5: updated $\mu_{i,V_p} \forall i \in V_c$, $p = 1, \dots, q$ following (18)
 - 6: **return** U^r , $\{m_p, p = 1, \dots, q\}$
-

Algorithm 3 agglomerative clustering

- 1: Let $V_p = i \forall i = 1, \dots, n$ and let $\mathfrak{V} = \{V_p\}$ where $p = 1, \dots, n$
 - 2: **while** $|\mathfrak{V}| \geq q$ **do**
 - 3: Select cluster-pair (V_p, V_g) based on (23)
 - 4: $V_{p^*} = V_p \cup V_g$
 - 5: $\mathfrak{V}^* = \mathfrak{V} \cup V_{p^*} \setminus \{V_p, V_g\}$
 - 6: **return** set of customer clusters \mathfrak{V}^*
-

Table 6: Comparison of solution quality between DRI and HGS-TW for different runtimes - instance size: 600

Θ	15		30		45		60		75		90		120		300	
	DRI	HGS	DRI	HGS	DRI	HGS	DRI	HGS	DRI	HGS	DRI	HGS	DRI	HGS	DRI	HGS
C1_6_1	14,600	14,095	14,600	14,095	14,600	14,095	14,600	14,095	14,600	14,095	14,600	14,095	14,600	14,095	14,600	14,095
C1_6_10	14,103	14,003	13,970	13,772	13,963	13,772	13,964	13,772	13,943	13,714	13,939	13,713	13,937	13,710	13,919	13,686
C1_6_4	13,989	14,129	13,905	13,873	13,867	13,703	13,838	13,676	13,827	13,676	13,811	13,674	13,801	13,660	13,752	13,618
C1_6_6	14,399	14,089	14,399	14,089	14,399	14,089	14,400	14,089	14,399	14,089	14,399	14,089	14,399	14,089	14,399	14,089
C2_6_1	8,266	8,029	8,241	7,776	8,241	7,776	8,241	7,776	8,241	7,776	8,241	7,776	8,241	7,776	8,239	7,774
C2_6_10	7,573	7,593	7,480	7,229	7,482	7,190	7,465	7,177	7,465	7,175	7,465	7,174	7,464	7,170	7,441	7,165
C2_6_4	7,306	7,323	7,180	7,018	7,145	6,949	7,132	6,947	7,125	6,930	7,123	6,928	7,120	6,921	7,112	6,908
C2_6_6	8,141	7,729	7,924	7,530	7,922	7,486	7,914	7,486	7,912	7,479	7,906	7,479	7,883	7,475	7,880	7,471
R1_6_1	22,345	22,453	22,070	22,049	21,989	21,896	21,987	21,856	21,903	21,785	21,813	21,745	21,813	21,661	21,712	21,431
R1_6_10	18,542	18,445	18,305	18,298	18,264	18,218	18,181	18,077	18,111	18,047	18,064	18,041	17,984	17,862	17,840	17,756
R1_6_4	16,420	16,709	16,358	16,359	16,271	16,292	16,265	16,220	16,260	16,218	16,193	16,206	16,101	16,167	15,949	15,994
R1_6_6	18,825	18,859	18,630	18,696	18,564	18,632	18,505	18,560	18,456	18,492	18,427	18,435	18,399	18,358	18,218	18,132
R2_6_1	15,812	15,866	15,618	15,540	15,510	15,433	15,455	15,369	15,453	15,302	15,438	15,287	15,437	15,248	15,343	15,200
R2_6_10	12,704	12,627	12,295	12,423	12,319	12,290	12,238	12,196	12,152	12,145	12,139	12,118	12,109	12,031	12,109	11,890
R2_6_4	8,293	8,275	8,163	8,174	8,111	8,130	8,117	8,090	8,105	8,046	8,087	8,015	8,053	7,986	8,063	7,965
R2_6_6	12,692	12,810	12,392	12,450	12,383	12,406	12,336	12,294	12,298	12,291	12,252	12,261	12,193	12,220	12,116	12,061
RC1_6_1	17,887	17,982	17,642	17,778	17,666	17,629	17,578	17,509	17,478	17,422	17,469	17,350	17,407	17,319	17,294	17,141
RC1_6_10	16,425	16,467	16,171	16,341	16,149	16,224	16,073	16,153	16,064	16,103	16,044	16,086	15,967	16,021	15,865	15,924
RC1_6_4	15,383	15,471	15,242	15,344	15,224	15,240	15,174	15,179	15,152	15,128	15,094	15,095	14,993	15,031	14,963	14,928
RC1_6_6	17,340	17,316	17,082	17,008	17,145	16,974	17,046	16,872	16,868	16,872	16,834	16,865	16,799	16,786	16,704	16,631
RC2_6_1	12,511	12,598	12,350	12,360	12,265	12,226	12,236	12,121	12,230	12,072	12,224	12,047	12,201	12,027	12,191	12,011
RC2_6_10	9,361	9,540	9,250	9,327	9,263	9,235	9,209	9,194	9,182	9,151	9,180	9,140	9,172	9,081	9,111	9,021
RC2_6_4	7,492	7,586	7,308	7,417	7,281	7,278	7,245	7,188	7,217	7,138	7,198	7,132	7,178	7,100	7,165	6,995
RC2_6_6	11,504	11,460	11,232	11,238	11,194	11,195	11,150	11,076	11,085	11,022	11,068	11,006	11,053	10,936	11,042	10,852

Table 7: Comparison of solution quality between DRI and HGS-TW for different runtimes - instance size: 800

Θ	15		30		45		60		75		90		120		300	
	DRI	HGS	DRI	HGS	DRI	HGS	DRI	HGS	DRI	HGS	DRI	HGS	DRI	HGS	DRI	HGS
C1_8_1	25,184	25,184	25,184	25,184	25,184	25,184	25,184	25,184	25,184	25,184	25,184	25,184	25,184	25,184	25,184	25,184
C1_8_10	24,656	25,121	24,427	24,914	24,378	24,576	24,349	24,576	24,299	24,485	24,295	24,423	24,269	24,368	24,209	24,271
C1_8_4	24,410	25,051	24,264	24,586	24,283	24,467	24,170	24,389	24,143	24,317	24,094	24,287	24,066	24,259	23,978	24,024
C1_8_6	25,163	25,160	25,162	25,160	25,162	25,160	25,162	25,160	25,162	25,160	25,162	25,160	25,162	25,160	25,162	25,160
C2_8_1	12,063	12,065	12,049	11,665	12,049	11,662	12,049	11,662	12,049	11,662	12,049	11,662	12,049	11,662	12,049	11,662
C2_8_10	11,861	12,424	11,421	11,688	11,378	11,235	11,283	11,107	11,232	11,052	11,208	11,043	11,188	11,023	11,160	11,004
C2_8_4	11,461	11,848	11,083	11,290	11,054	11,056	11,034	11,006	11,011	10,934	10,996	10,848	10,985	10,762	10,936	10,720
C2_8_6	12,027	12,376	11,623	11,472	11,591	11,377	11,577	11,356	11,544	11,356	11,577	11,354	11,573	11,349	11,573	11,347
R1_8_1	38,179	39,765	37,689	38,715	37,513	38,041	37,484	37,819	37,460	37,787	37,416	37,752	37,341	37,457	37,172	37,140
R1_8_10	32,545	32,886	32,415	32,619	32,140	32,406	32,003	32,305	31,877	32,171	31,759	32,125	31,658	32,085	31,476	31,740
R1_8_4	29,182	29,365	28,914	29,250	28,908	29,047	28,761	29,047	28,719	28,982	28,684	28,842	28,599	28,726	28,182	28,169
R1_8_6	32,697	32,987	32,453	32,789	32,361	32,570	32,309	32,466	32,131	32,388	32,103	32,388	31,947	32,078	31,604	31,840
R2_8_1	26,626	27,772	26,038	26,560	25,866	25,995	25,818	25,693	25,783	25,554	25,695	25,553	25,550	25,452	25,403	25,152
R2_8_10	21,753	21,629	21,006	21,141	20,917	20,948	20,790	20,886	20,700	20,764	20,582	20,728	20,616	20,596	20,503	20,119
R2_8_4	14,066	14,528	13,873	14,161	13,779	13,947	13,707	13,840	13,656	13,781	13,569	13,741	13,525	13,720	13,433	13,430
R2_8_6	21,442	21,854	20,818	21,218	20,794	21,118	20,635	20,928	20,591	20,698	20,578	20,609	20,494	20,519	20,175	20,171
RC1_8_1	31,275	31,837	30,970	31,597	30,907	31,437	30,839	31,253	30,768	30,983	30,721	30,961	30,667	30,867	30,408	30,569
RC1_8_10	29,355	29,657	29,121	29,325	29,062	29,152	29,022	29,130	28,953	29,029	28,890	29,008	28,738	28,867	28,518	28,577
RC1_8_4	27,685	27,959	27,393	27,699	27,432	27,532	27,379	27,429	27,282	27,360	27,255	27,336	27,097	27,182	26,983	26,951
RC1_8_6	30,531	30,876	30,330	30,614	30,060	30,457	30,011	30,423	29,909	30,213	29,914	30,193	29,782	30,035	29,629	29,777
RC2_8_1	20,551	21,316	19,946	20,127	19,941	19,954	19,785	19,817	19,704	19,607	19,701	19,498	19,667	19,435	19,617	19,318
RC2_8_10	15,697	15,626	15,094	15,057	15,039	15,005	15,098	14,827	14,911	14,741	14,911	14,666	14,894	14,615	14,731	14,539
RC2_8_4	11,785	11,985	11,518	11,704	11,428	11,518	11,399	11,442	11,369	11,341	11,354	11,302	11,343	11,231	11,248	11,100
RC2_8_6	18,524	19,154	17,873	18,228	17,824	17,880	17,709	17,648	17,621	17,597	17,611	17,518	17,549	17,435	17,503	17,273

Table 8: Comparison of solution quality between DRI and HGS-TW for different runtimes - instance size: 1000

Θ	15		30		45		60		75		90		120		300	
	DRI	HGS	DRI	HGS	DRI	HGS	DRI	HGS	DRI	HGS	DRI	HGS	DRI	HGS	DRI	HGS
C1_10_1	42,499	42,479	42,499	42,479	42,499	42,479	42,499	42,479	42,499	42,479	42,499	42,479	42,499	42,479	42,499	42,479
C1_10_10	41,440	42,629	41,038	41,853	40,996	41,596	40,856	41,596	40,846	41,435	40,878	41,375	40,660	41,234	40,288	40,884
C1_10_4	40,721	42,189	40,447	41,490	40,423	41,387	40,365	41,135	40,160	41,019	40,173	41,019	40,045	41,019	39,743	40,138
C1_10_6	42,492	42,499	42,491	42,473	42,491	42,471	42,491	42,471	42,491	42,471	42,491	42,471	42,491	42,471	42,491	42,471
C2_10_1	17,837	19,065	17,440	17,404	17,437	17,331	17,437	16,879	17,437	16,879	17,437	16,879	17,437	16,879	17,437	16,879
C2_10_10	16,835	19,317	16,173	17,532	16,079	16,700	16,056	16,366	16,012	16,067	15,996	15,990	15,987	15,850	15,943	15,802
C2_10_4	16,879	18,076	15,912	17,300	15,901	16,727	15,825	16,428	15,688	15,904	15,783	15,838	15,681	15,632	15,611	15,541
C2_10_6	17,390	19,038	16,758	16,827	16,725	16,550	16,695	16,398	16,680	16,385	16,668	16,365	16,668	16,346	16,661	16,336
R1_10_1	57,588	291,558	56,175	291,558	55,729	291,558	55,506	291,558	55,393	56,086	55,169	55,530	55,052	55,227	54,461	54,706
R1_10_10	50,181	50,389	49,635	50,322	49,793	49,939	49,532	49,667	49,242	49,406	49,194	49,217	48,914	49,160	48,360	48,776
R1_10_4	44,620	45,312	44,490	44,720	44,434	44,548	44,349	44,448	44,291	44,297	44,153	44,297	43,786	44,123	43,272	43,624
R1_10_6	49,909	50,374	49,765	49,985	49,496	49,827	49,221	49,656	49,393	49,603	49,187	49,331	48,968	49,176	48,264	48,662
R2_10_1	39,652	41,491	38,777	39,546	38,420	38,719	38,359	38,474	38,150	38,097	37,936	38,012	37,868	37,735	37,447	37,291
R2_10_10	32,690	33,478	31,937	32,070	31,801	31,794	31,487	31,575	31,328	31,377	31,262	31,182	31,148	31,044	30,771	30,640
R2_10_4	19,561	20,050	19,112	19,599	19,129	19,275	19,001	19,093	18,675	19,093	18,740	18,999	18,566	18,784	18,372	18,347
R2_10_6	32,019	32,675	31,335	32,070	30,998	31,450	30,867	31,172	30,639	30,997	30,619	30,753	30,364	30,590	30,113	30,306
RC1_10_1	48,414	48,767	48,085	48,404	47,659	48,053	47,455	48,053	47,579	47,876	47,348	47,839	47,345	47,483	46,889	47,119
RC1_10_10	45,715	46,431	45,401	45,829	45,129	45,646	45,062	45,454	45,020	45,400	44,826	45,251	44,699	44,969	44,296	44,480
RC1_10_4	43,278	43,517	42,952	43,417	42,857	43,319	42,786	43,243	42,705	43,117	42,697	43,065	42,501	42,979	42,156	42,414
RC1_10_6	47,526	47,981	46,856	47,312	46,940	47,059	46,654	46,816	46,658	46,603	46,408	46,603	46,327	46,548	45,720	46,048
RC2_10_1	30,590	34,143	29,631	31,718	29,376	30,520	29,206	30,164	29,158	29,856	29,054	29,461	29,034	28,988	28,725	28,426
RC2_10_10	23,877	24,454	23,086	23,574	22,980	22,942	22,884	22,933	22,765	22,704	22,668	22,675	22,477	22,579	22,303	22,109
RC2_10_4	17,081	17,900	16,665	17,500	16,528	16,901	16,500	16,714	16,418	16,655	16,362	16,543	16,294	16,351	16,059	16,031
RC2_10_6	28,476	30,474	27,305	29,121	26,966	27,981	26,976	27,465	26,874	27,106	26,779	26,991	26,611	26,634	26,378	26,205

References

- Accorsi L, Vigo D (2021) A fast and scalable heuristic for the solution of large-scale capacitated vehicle routing problems. *Transportation Science* 55(4):832–856.
- Anderberg MR (1973) *Cluster Analysis for Applications* (Academic Press, New York).
- Arnold F, Gendreau M, Sörensen K (2019) Efficiently solving very large-scale routing problems. *Computers & Operations Research* 107:32–42.
- Arnold F, Santana Í, Sörensen K, Vidal T (2021) PILS: Exploring high-order neighborhoods by pattern mining and injection. *Pattern Recognition* 116:107957.
- Arnold F, Sörensen K (2019) Knowledge-guided local search for the vehicle routing problem. *Computers & Operations Research* 105:32–46.
- Battarra M, Erdoğan G, Vigo D (2014) Exact algorithms for the clustered vehicle routing problem. *Operations Research* 62(1):58–71.
- Beek O, Raa B, Dullaert W, Vigo D (2018) An efficient implementation of a static move descriptor-based local search heuristic. *Computers & Operations Research* 94:1–10.
- Bent R, Van Hentenryck P (2010) Spatial, temporal, and hybrid decompositions for large-scale vehicle routing with time windows. Cohen D, ed. *Principles and Practice of Constraint Programming*. (Springer, Berlin Heidelberg), 99–113.
- Bezdek JC (1981) *Pattern Recognition with Fuzzy Objective Function Algorithms* (Springer US, Boston).
- Bräysy O, Gendreau M (2005) Vehicle routing problem with time windows, Part I: Route construction and local search algorithms. *Transportation Science* 39(1):104–118.
- Clarke G, Wright JW (1964) Scheduling of vehicles from a central depot to a number of delivery points. *Operations Research* 12(4):568–581.
- Costa L, Contardo C, Desaulniers G (2019) Exact branch-price-and-cut algorithms for vehicle routing. *Transportation Science* 53(4):946–985.
- Dantzig GB, Ramser JH (1959) The truck dispatching problem. *Management Science* 6(1):80–91.
- Ewbank H, Wanke P, Hadi-Vencheh A (2016) An unsupervised fuzzy clustering approach to the capacitated vehicle routing problem. *Neural Computing and Applications* 27(4):857–867.
- Fisher ML, Jaikumar R (1981) A generalized assignment heuristic for vehicle routing. *Networks* 11(2):109–124.
- Gehring H, Homberger J (1999) A parallel hybrid evolutionary metaheuristic for the vehicle routing problem with time windows. Miettinen K, Mäkelä M, Toivanen J, eds. *Proc. EUROGEN99* (University of Jyväskylä, Finland, Finland), 57–64.
- Gillett BE, Miller LR (1974) A heuristic algorithm for the vehicle-dispatch problem. *Operations Research* 22(2):340–349.
- Helsgaun K (2000) An effective implementation of the Lin–Kernighan traveling salesman heuristic. *European Journal of Operational Research* 126(1):106–130.
- Jain AK (2010) Data clustering: 50 years beyond k-means. *Pattern Recognition Letters* 31(8):651–666.
- Kool W, Juninck JO, Roos E, Cornelissen K, Agterberg P, van Hoorn J, Visser T (2022) Hybrid genetic search for the vehicle routing problem with time windows: A high-performance implementation. *12th DIMACS Implementation Challenge Workshop*.
- Lin S, Kernighan BW (1973) An effective heuristic algorithm for the traveling-salesman problem. *Operations Research* 21(2):498–516.
- Park HS, Jun CH (2009) A simple and fast algorithm for k-medoids clustering. *Expert Systems with Applications* 36(2):3336–3341.
- Qi M, Lin WH, Li N, Miao L (2012) A spatiotemporal partitioning approach for large-scale vehicle routing problems with time windows. *Transportation Research Part E: Logistics and Transportation Review* 48(1):248–257.
- Ropke S, Pisinger D (2006) An adaptive large neighborhood search heuristic for the pickup and delivery problem with time windows. *Transportation Science* 40(4):455–472.
- Sahin MK, Yaman H (2022) A branch and price algorithm for the heterogeneous fleet multi-depot multi-trip vehicle routing problem with time windows. *Transportation Science* 56(6):1636–1657.
- Santini A, Schneider M, Vidal T, Vigo D (2023) Decomposition strategies for vehicle routing heuristics. *INFORMS Journal on Computing* 35(3):543–559.
- Schneider M, Stenger A, Schwahn F, Vigo D (2015) Territory-based vehicle routing in the presence of time-window constraints. *Transportation Science* 49(4):732–751.
- Solomon MM (1987) Algorithms for the vehicle routing and scheduling problems with time window constraints. *Operations Research* 35(2):254–265.
- Toth P, Vigo D (2003) The granular tabu search and its application to the vehicle routing problem. *INFORMS Journal on Computing* 15(4):333–346.
- Toth P, Vigo D (2014) *Vehicle Routing: Problems, Methods, and Applications*, 2nd ed. (Society for Industrial and Applied Mathematics, Philadelphia).
- Vidal T, Crainic TG, Gendreau M, Lahrichi N, Rei W (2012) A hybrid genetic algorithm for multidepot and periodic vehicle routing problems. *Operations Research* 60(3):611–624.

- Vidal T, Crainic TG, Gendreau M, Prins C (2013) A hybrid genetic algorithm with adaptive diversity management for a large class of vehicle routing problems with time-windows. *Computers & Operations Research* 40(1):475–489.
- Vidal T, Laporte G, Matl P (2020) A concise guide to existing and emerging vehicle routing problem variants. *European Journal of Operational Research* 286(2):401–416.
- Wong KF, Beasley JE (1984) Vehicle routing using fixed delivery areas. *Omega* 12(6):591–600.
- Yücenur GN, Demirel NÇ (2011) A new geometric shape-based genetic clustering algorithm for the multi-depot vehicle routing problem. *Expert Systems with Applications* 38(9):11859–11865.